universität wien

MASTERARBEIT / MASTER'S THESIS

Titel der Masterarbeit / Title of the Master 's Thesis

'Patient-derived organoids as a model for investigating epigenetic basis of radio-resistance in rectal cancer'

verfasst von / submitted by

Ajna Logo

angestrebter akademischer Grad / in partial fulfilment of the requirements for the degree of

Master of Science (MSc)

Wien, 2022 / Vienna, 2022

Studienkennzahl lt. Studienblatt / degree programme code as it appears on the student record sheet:	UA 066 830
Studienrichtung lt. Studienblatt / degree programme as it appears on the student record sheet:	Master's degree programme Molecular Microbiology, Microbial Ecology and Immunobiology
Betreut von / Supervisor:	Prof. Dr. Gerda Egger

Acknowledgments

First and foremost, I wish to thank Prof. Dr. Gerda Egger for all the support during my Master's Thesis. Thank you for allowing me to prove myself, for all the suggestions, inspiring discussions, and motivation. Special thanks to my dearest and best supervisor, Loan Tran, MSc. Thank you for selflessly sharing your knowledge and experience with me, and for all motivating talks about both science and life. Besides being the best supervisor that I could imagine, you have become my lifetime friend. I am thankful for getting the opportunity to have supervisors who inspire me both as a scientist and as a person.

Furthermore, many thanks to the entire Gerda Egger's Lab and Ludwig Boltzmann Institute Applied Diagnostics for being great colleagues and friends. Thanks to you and the work environment that we had, I was always looking forward to my next working day. I am sure that being a part of this amazing collective, with the best supervision I could have, marked my entire career life, pushing my motivation and ambition further. I also want to thank everyone from the Department of Pathology, Division of Nuclear Medicine, and Department of Radiation Oncology, Medical University of Vienna, who helped me during my work.

I also have to thank my dearest friend, Kristina Draganic, for believing in me in the very beginning, and for living through together every good and bad day that we have had.

None of this would be possible without my friends and family. I am the luckiest person to have all of you standing by my side selflessly, being so proud of my every success. Even if we are kilometers apart, it is much easier to make big steps and achievements, but also mistakes, when I know that so many people are loving me and supporting me. Special thanks to my Deni, for giving me endless love and support over the past years. Thank you for being involved so much in my project, for discussing with me scientific papers and experiments, and for trying your best to understand everything I talked about. Most importantly, I owe the biggest thanks to my parents and brother who always supported me unconditionally. You all showed me what it means to fight for yourself but to remain a good person. Mom and dad, thank you for all the life lessons, being my best friends and my role models throughout my life.

Table of Contents

Abstract

Colorectal cancer (CRC) is one of the most common causes of cancer deaths worldwide. Around 30% of all CRC cases occur in the rectum. Typical care for patients with locally advanced rectal cancer is neoadjuvant chemoradiation followed by surgery. However, only 15–20% of rectal cancer patients have a pathological Complete Response (pCR) to neoadjuvant chemoradiation therapy. The others have no clinical benefit, and they suffer from the negative consequences of toxicities and surgical delays. We are using patient-derived organoids (PDOs) from rectal cancer patients to study the predisposing epigenetic mechanisms of radiotherapy response. Vice versa, we want to investigate the effects of ionizing radiation on the epigenome. Additionally, we hypothesize that treatment using Decitabine (DAC, DNMT inhibitor) and radiotherapy together is beneficial. Therefore, we want to study their combinational effect further.

While the overall project aims to address three different goals, the Master's Thesis Project aimed to perform all necessary experiments, which are highly important for setting up the stage for further investigation. Therefore, I sought to determine the sensitivity of PDO lines towards Decitabine and radiotherapy and perform pilot experiments on how radiotherapy affects global DNA methylation levels. Finally, I carried out experiments that tackled the possible effects and benefits of combinational treatment compared to single therapies. Besides, I have successfully established a potentially radio-persistent organoid line, adding a new aspect to the entire project. Most importantly, my results indicate an existing effect of radiotherapy on DNA methylation.

Zusammenfassung

Darmkrebs (CRC) ist weltweit eine der häufigsten Todesursachen durch Krebs. Etwa 30 % aller CRC-Fälle treten im Rektum auf. Die typische Behandlung von PatientInnen mit lokal fortgeschrittenem Rektumkarzinom ist eine neoadjuvante Radiochemotherapie gefolgt von einer Operation. Allerdings zeigen nur 15–20 % der PatientInnen mit Rektumkarzinom ein pathologisches vollständiges Ansprechen (pCR) auf eine neoadjuvante Radiochemotherapie. Andere PatientInnen haben keinen klinischen Nutzen und leiden unter den negativen Folgen von Toxizitäten und chirurgischen Verzögerungen. Wir verwenden Patient-derived Organoids (PDOs) etabliert aus Gewebe von RektalkrebspatientInnen, um die prädisponierenden epigenetischen Mechanismen des Strahlentherapie-Ansprechens zu untersuchen. Umgekehrt wollen wir die Auswirkungen ionisierender Strahlung auf das Epigenom untersuchen. Darüber hinaus stellen wir die Hypothese auf, dass die Behandlung mit Decitabine (DAC, DNMT-Inhibitor) und Strahlentherapie zusammen vorteilhaft ist. Daher wollen wir ihre Kombinationswirkung weiter untersuchen.

Während das Gesamtprojekt auf drei verschiedene Ziele abzielt, zielte das Masterarbeitsprojekt darauf ab, alle notwendigen Experimente durchzuführen, die sehr wichtig sind, um die Voraussetzungen für weitere Untersuchungen zu schaffen. Daher habe ich versucht, das Ansprechen von PDO-Linien gegenüber Decitabin und Strahlentherapie zu bestimmen und Pilotversuche durchzuführen, die untersuchen wie Strahlentherapie die globale DNA-Methylierung beeinflusst. Schließlich führte ich Experimente durch, die sich mit den möglichen Wirkungen und Vorteilen einer Kombinationsbehandlung im Vergleich zu Einzeltherapien befassten. Außerdem habe ich erfolgreich eine potenziell strahlenbeständige Organoidlinie etabliert, die dem gesamten Projekt einen neuen Aspekt hinzufügt. Am wichtigsten ist, dass meine Ergebnisse auf eine bestehende Wirkung der Strahlentherapie auf die DNA-Methylierung hinweisen.

Introduction

Colorectal cancer (CRC)

Colorectal cancer (CRC) is the third most common cancer and the third leading cause of cancer death in Austria [1]. Despite the introduction of screening programs, the incidence of CRC has been increasing in most European countries, especially among individuals younger than 50 years. This trend may be caused by different factors and bad lifestyle choices, including increased alcohol consumption, lack of exercise, and high prevalence of obesity [2]. Other recognized risk factors include family history and diabetes mellitus. However, most CRC cases are sporadic, and only one-quarter of patients have related family anamnesis. Therefore, bad nutritional habits and lifestyle factors are leading risks of colorectal cancers, especially among young adults, who face more advanced disease and unfavorable prognoses. CRC is predominant in western, more-developed regions of the world [3,4].

In 2015, Guinney et al. proposed a CRC classification system and four different groups - CMS1-4 [5]. These four CRC subtypes differ on the genomic, transcriptomic, and epigenomic levels [5–7]. CMS1 subtype is hypermutated and characterized by a DNA mismatch repair (MMR) defect. Additionally, this subtype is frequently characterized by BRAF mutation and is usually located in the proximal part of the colon [6,7]. CMS2 subtype is characterized by activation of WNT, MYC, and TGFβ pathway. Furthermore, this CRC subtype was shown to have a higher number of oncogenes. Importantly, these tumors show high epithelial differentiation [6,7]. KRAS mutations and distinct metabolic features more often characterize CMS3 tumors [7]. Finally, the distally located CMS4 subtype is represented by upregulation of epithelial-mesenchymal transition (EMT) and stromal invasion [5].

Colorectal cancer arises due to the accumulation of genetic mutations and epigenetic alterations that affect multiple molecular pathways, leading to molecular heterogeneity responsible for high variability in response to anti-cancer therapies [6,7]. Previously mentioned CRC subtypes (CMS1-4) are also characterized by distinct epigenetic features [7]. For example, CMS1 tumors show a high CpG island methylation phenotype (CIMP-high) and are associated with hypermethylation of important genes, such as *MLH1*. As mentioned before, they are linked to microsatellite instability (MSI) and MMR deficiency [6,7]. The MMR system deficit can be caused by a genetic mutation in *MLH1* and the mentioned promoter hypermethylation of this gene [7]. Other subtypes (CMS2-4) show high chromosomal instability (CIN) and are altogether known as CIN tumors, which show a high rate of alterations of large portions of chromosomes. Additionally, these subtypes show CIMP-low phenotypes [5–7].

Rectal cancer

One-third of all annual CRC cases in the European Union occur in the rectum [8]. Rectal cancer subtypes are characterized by different genetic and epigenetic alterations that slightly differ from colon cancer [9,10]. Additionally, rectal cancer patients have a higher risk of recurrence, and most of them do not show sufficient response to therapy [9,11]. Rectal cancers usually develop via the chromosomal instability (CIN) pathway and have a high frequency of *TP53* mutations. Some cases can be caused by a deficiency in mismatch repair (dMMR). Like other distal-located CRC cases, rectal cancer is usually not characterized by CIMP-high phenotype [10].

Despite showing unique tumor markers, rectal cancer is usually not recognized as an independent tumor entity [10]. Therefore, almost no molecular markers are available to predict therapy response or evaluate whether a specific therapeutical approach would be convenient for rectal cancer patients [9–11]. Furthermore, literature already suggested and showed that rectal cancer shows a great intra- and inter-tumoral heterogeneity that is still not sufficiently explored [9,11]. Scientists have already suggested intra-tumoral heterogeneity to affect the diverse therapy response among rectal-cancer patients. However, this is yet to be further investigated and validated [9,11]. Taken all together, it is of high importance to develop improved diagnostic tools and treatment options specific for rectal cancer.

Radiotherapy

Locally advanced rectal cancer (LARC) is typically treated with neoadjuvant chemoradiation (CRT) followed by surgery and pathological assessment [12,13]. Thus, for the management of rectal cancer, multidisciplinary teams are pivotal [12]. Radiotherapy uses ionizing radiation to induce single-strand, double-strand breaks, and reactive oxygen species (ROS). Altogether, this leads to DNA damage and cell death in cancer cells [13].

CRT implies a total radiation dose of 45-50 Gy given in about 25 fractions. This treatment is replaced with neoadjuvant short-course radiotherapy among patients that are intolerable towards chemoradiation. In this case, a total dose of 25 Gy is delivered during one week (5 x 5 Gy). However, this causes a decrease in the pathological Complete Response (pCR) rate [14]. Over 80% of patients do not achieve pCR after the standard chemoradiation approach [5]. Therefore, several strategies were explored to improve this low response rate. Many chemotherapeutic therapies and different radiation doses have been tested so far. However, all other approaches were too toxic for patients [13,14].

Altogether, treatment resistance remains a significant challenge, and there is a need to identify and develop successful radiosensitizers that would improve response to radiation. Currently, there are no approved radiosensitizers currently used in the clinic.

Bob Weinberg and Douglas Hanahan proposed the "Hallmarks of Cancer" in 2000, describing cellular features shared between cancer cells despite their apparent diversity [15]. Initially, six originally proposed hallmarks were first expanded in 2011 when four additional characteristics were included in this fundamental framework of cancer biology [16]. Resistance to radiotherapy is associated with several biological alterations, including alterations in the cell cycle, tissue invasion, evading cell death, etc. The literature suggests that alterations in all the hallmarks of cancer are essential in developing radioresistant phenotypes. Therefore, targeting a combination of hallmarks could be beneficial in the resensitization of patients [13].

Epigenetic mechanisms in CRC

Epigenetics refers to heritable changes in DNA expression that are not caused by the changes in the DNA sequence itself [17]. Epigenetic mechanisms were shown to have a central role in the development, progression, and pathogenesis of various cancers, which is also the case with CRC [6]. Therefore, besides DNA methylation itself, other epigenetic mechanisms, such as different histone modifications and ncRNAs, have been linked to colorectal cancer pathogenesis and are under investigation as potential therapeutic targets [6]. Importantly, exploring single epigenetic mechanisms and their role in carcinogenesis is insufficient due to the critical crosstalk in-between [6]. Previously mentioned Hallmarks of Cancer were further expanded in 2022, when additional emerging hallmarks and enabling characteristics were included. Importantly, 'nonmutational epigenetic reprogramming' was included in this framework, emphasizing the importance of epigenetic mechanisms, and indicating that epigenetics might have been neglected so far and more research needs to be done in future [18].

Additionally, epigenetic marks were shown to be a great promise as biomarkers. Many of them have already been suggested to be relevant for diagnostic, prognostic, and predictive purposes in all tumor entities, including CRC [6,19,20]. For example, Septin 9 (SEPT9, a GTP-binding protein) is an FDA-approved non-invasive DNA methylation biomarker used for CRC screening [6]. Likewise, *MLH1* DNA methylation in CRC, which causes the MMR deficiency, is the biomarker commonly used in clinics as a strategy for distinguishing patients with Lynch syndrome and sporadic CRCs [6].

Finally, since epigenetic alterations are reversible, epigenetic therapy is under investigation, and more and more epigenetic drugs are developed [6]. Preclinical studies suggest that epigenetic modifiers might have synergistic activity when combined with other anti- cancer drugs. Therefore, the future goal is to investigate how these drugs can be used as potential resensitizers of standard therapies such as chemotherapy, radiotherapy, and immunotherapy [6,21–24].

DNA methylation in CRC

DNA methylation is the epigenetic mechanism that occurs at the C5 position at CpG dinucleotides in mammals, where a methyl group (CH3) is being added [17]. This is known to be a silencing mechanism that is maintained due to the presence of DNA methyltransferases (DNMTs). In this way, our genome silences transposable and human endogenous retroviral elements and represses the transcription of specific genes [17].

Carcinogenesis leads to the local hypermethylation of particular gene promoters that are typically important for tumor suppression [17]. For example, in CRC, many important tumor-suppressors, such as *APC* and *MLH1*, are known to be often hypermethylated and consequently silenced. In addition, CpG islands (200-2,000 nucleotide long CpG-rich regions that are evolutionary kept unmethylated) are often hypermethylated [6,17].

On the other hand, global hypomethylation is mainly related to the loss of methylation in repetitive elements, which comprise a large portion of the human genome (~45%). Highly significant in terms of DNA methylation are Alu and LINE1 elements, which together comprise about 30% of the genome. In healthy cells, they remain heavily methylated to prevent their transcription [17,25]. If hypomethylated and activated, LINE1 elements can act as retrotransposons, leading to genomic instability. However, their hypomethylation is a characteristic of cancer cells . Since they comprise a significantly large part of our genome, analysis of the methylation status of LINE1 elements can be used as a marker in the estimation of global DNA methylation levels [25].

DNA methyltransferase inhibitors 5-azacytidine (azacytidine) and 2'-deoxy-5-azacytidine (decitabine) are FDA-approved drugs for treating myelodysplastic syndrome (MDS) [6,17,26]. They act as nucleoside analogues that incorporate into DNA, which leads to trapping of the DNMT enzyme and its degradation. Consequently, methylation marks are passively lost, leading to demethylation, reverting the hypermethylation, and reactivating essential tumor suppressor genes crucial in controlling proliferation and apoptosis pathways [26]. Considering their mode of action, they are active only during the S-phase of the cell cycle [17]. However, both DNMTis are deemed to be unstable [17,26]. The resistance to these DNMTis is related to the expression levels of the proteins that are important for their uptake and cellular transport mechanisms, such as transporter ENT-1, which studies already showed to be essential for sensitivity towards decitabine [26]. Additionally, since DNMTis have to be further metabolically processed to get activated, several steps can be found to be altered in case of resistance [17,26].

Rectal cancer is suggested to have unique DNA methylation aberrations that are tumor-specific and may be successfully used as biomarkers [9]. In 2015, Exner et al. identified new diagnostic DNA methylation biomarker sets that were shown to distinguish between tumor and peripheral blood/adjacent tissue successfully [10]. It was also suggested that alterations in genomic methylation patterns are related to the radiosensitivity of cancer cells. Epigenetic silencing of essential tumor suppressor genes is believed to have a central role in developing radioresistant phenotype and

aberrations in crucial pathways that cause it. Literature has already suggested that the use of DNMT inhibitors, such as DAC, may be beneficial in enhancing the radiosensitivity of cancer cells [10,27].

On the other hand, ionizing radiation seems to have direct effects (e.g., DNA damage, cell killing), leading to indirect impacts, including epigenomic alterations, such as DNA methylation. However, the literature suggests that changes in DNA methylation depend on various factors, including dose, time, and type of radiation. Also, changes were tissue-specific and dependent a lot on post-irradiation time [28,29].

Patient-derived organoids (PDOs) as *in vitro* preclinical models for rectal cancer

The recent development of organoid techniques has allowed us to precisely study many different diseases and processes in the human body [30–32]. Additionally, this technique overcomes all the shortcomings and bridges all the previously used technical gaps. For instance, despite all the advantages and extensive information animal models can provide, these models still do not entirely reflect human physiology. On the other hand, 2D cell cultures lack physiological complexity, which remains the limitation of this model system [30]. Patient-derived organoids are derived from self-organizing mammalian pluripotent or adult stem cells *in vitro* and grown in 3D [30,31]. They can recapitulate all critical features of the tissue of origin, including genetic alterations and drug response [30].

Therefore, organoid technology presents a valuable method with great potential in cancer research, tumor modeling, precision medicine development, and drug screening [31]. Several research groups have already established CRC organoids. CRC PDOs have been used to study drug resistance, metabolic processes, metastasis and to tackle many other research questions [31,32]. Importantly, literature has shown that the DNA methylation profile is stable in human intestinal epithelial organoids and further reflects the primary tumor's profile [33–35].

Gerda Egger's Lab has successfully derived organoid cultures from tumorigenic and adjacent healthy tissue obtained from the same patient diagnosed with CRC. The derived organoid cultures were characterized on a histopathological level and reproduced the grade and differentiation capacity of parental tumors.

Furthermore, the mutational and DNA methylation profile analysis confirmed that organoids highly reflect the patient's profile stably over several months of culture. Altogether, these results demonstrated that organoids could represent a high level of intertumoral heterogeneity.

Conclusively, data obtained within our lab confirms a high potential of PDOs and their great promise for personalized cancer medicine. Accumulating evidence indicates that PDOs can predict drug and therapy responses in the clinic, including the response to chemoradiation in advanced rectal cancer. PDOs have already been used to investigate and predict sensitivity towards radiotherapy, and it was shown that one could successfully distinguish between sensitive and resistant organoid lines [32,36].

Aims of the project and expected outcome

The Master thesis was part of a larger project lead by Loan Tran in the lab of Gerda Egger. We are using patient-derived organoids (PDOs) established from the rectal cancer patient tissue to investigate the probable effect of radiotherapy on the human epigenome and, vice versa, the predisposing epigenetic basis of radiotherapy response. Therefore, the first part of the project will examine the potential impact of ionizing radiation on DNA methylation. Next, we aim to evaluate the combinational effects of radiotherapy and Decitabine (DAC). DAC is a DNMT inhibitor (DNMTi), which was already suggested as a successful radiosensitizer. Therefore, we will lastly focus on rectal organoid lines that acquired radioresistance and subject them to epigenetic remodeling with DAC, testing DNMTis as radiosensitizers among our organoid lines. These findings will widen our knowledge and be the basis for the potential administration of combinatorial epigenetic treatment of patients suffering from rectal cancer. Graphical overview of these three explained aims is represented in *Figure 1*.

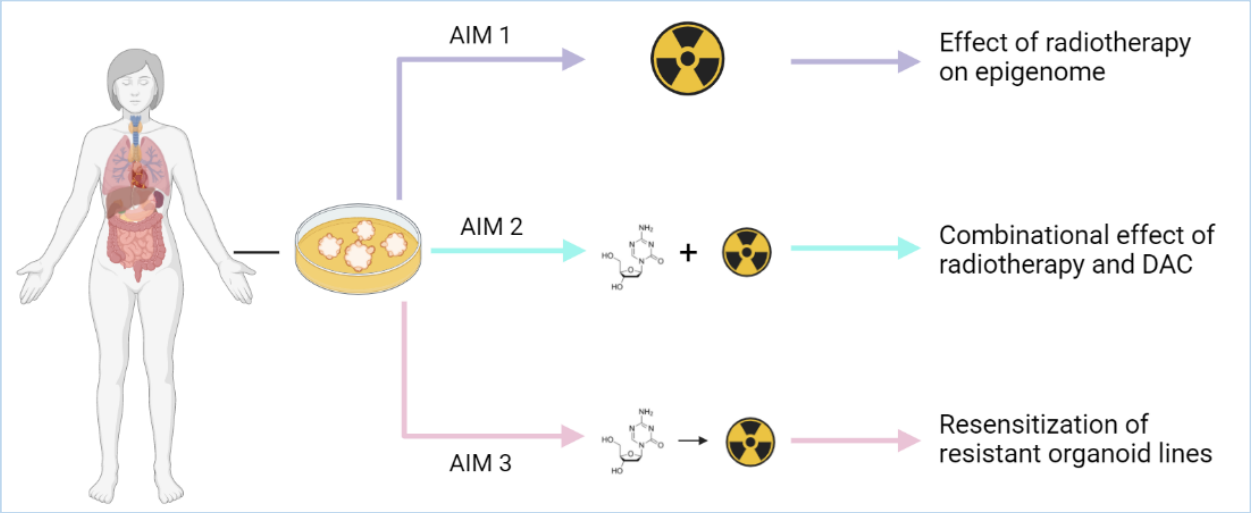

Figure 1. Overview of three aims of the project. *The project will investigate the missing link between radiotherapy and DNA methylation by exploring the effect of ionizing radiation on the epigenome through 'Aim 1'. Further, the last two aims will address the potential of combining the DAC and radiation treatment.*

Work packages of the Master Thesis Project

This project was newly started based on the data obtained within Loan Tran's PhD thesis and on literature research. Together, we designed the timeline for the project and handed in the grant application to secure the financing. All described aims above were planned in detail and will be further investigated in the following two years. However, to set the stage for further experiments,

my Master's Thesis Project aimed to perform all necessary experiments, which are highly important as the basis for investigating every previously explained aim.

Therefore, we determined the following work packages as being crucial to be done within my Master's Thesis:

- Determination of half-inhibitory concentration (IC50) of organoid lines towards DAC
- Determination of radiation response curves
- Pilot experiments aiming to investigate the effect of single or combinational treatments on DNA methylation in CRC PDOs

Material and Methods

Unless differently stated, all protocols were kindly provided by my supervisor, Loan Tran MSc.

Isolation of tumor cells from biopsies

The tumor tissue sample was washed several times using 1x DPBS (Gibco™, Cat. #14190144). The cleaned tissue part was placed in a 12-well plate (Buch & Holm A/S, Cat. #92012), all unwanted components were removed. The remaining piece was transferred to the next well, dissected into small pieces using scalpels, and resuspended with 1 mL of Cell Recovery Solution (Corning®, Cat. #354253) + 0.1% Y-27632, Rock inhibitor (SCM075 Sigma-Aldrich). This suspension was incubated at 37°C for at least 30 minutes. However, every 15 minutes, it was resuspended to induce better digestion. Additionally, we inspected the progress through an inverted microscope. When many single cells were visible, tissue was filtered into Falcon tubes through MACS® SmartStrainers to obtain a uniform single-cell suspension. Next, Falcon tubes were centrifuged at 1200 rpm/400 g for at least 5 minutes at room temperature (RT). This was followed by adding 1x DPBS and further centrifugation step with the same settings as before, aiming to wash the cell pellet and further reduce any chance of contamination. The washed cell pellet was resuspended in 1 mL ice-cold 1x DPBS and divided into 2 Falcon tubes. 1/5 of the suspension was seeded in 2-4 basement membrane matrix drops (each containing 30 µl of the matrix-cell mixture). The rest of the suspension was frozen in 3-4 cryotubes containing 600 µl Recovery™ Cell Culture Freezing Medium (Gibco™, Cat. #12648010). Cryotubes were first placed at – 80 °C in freezing containers to ensure a slow cooldown. After 24h, we transferred them to liquid nitrogen for long-term storage.

Cultivation of Patient-derived Organoids

Components of the medium used for patient-derived colorectal cancer organoids

Established organoid lines were cultivated in WENRAS medium, always freshly prepared following the instructions written in Table 1 and Table 2. We regularly monitored the growth of the organoids under the microscope. Whenever needed, the medium was discarded, and the new one was added carefully

Table 1. *Components of WENRAS medium*

WENRAS medium	**Stock**	**Final concentration**	
Wnt3A-CM	100x	50x	Maintenance and regeneration of stem cells
Basal medium	1x	1x	*See Table 2*.
R-spondin1-CM	100x	10x	Promotes canonical WNT/β-catenin signaling
B27 supplement	50x	1x	Neuronal cell culture supplement
N2 supplement	100x	1x	Serum-free supplement based on Bottenstein's N-1 formulation
Nicotinamide	1 M	10 mM	Vitamin B3 derivate, cell proliferation
N-acetyl-L-cysteine	500 mM	1 mM	Antioxidant, increases cellular pools of free radical scavengers
Noggin	100 µg/mL	100 ng/mL	Inhibitor of BMP (TGF-β family)
A8301	500 µg	500 nM	Inhibitor of ALK (TGF-β receptor family)
SB202190	10 mM	10 µM	Inhibitor of p38 MAP kinases
Y27632 Rock-inh.	100 mM	10 µM	Prevention of anoikis
Gastrin	100 µM	10 nM	Growth factor
EGF	0,5 mg/ml	50 ng/mL	Proliferation, differentiation, and survival

Table 2. *Components of Basal growth medium*

Basal growth medium (components added to Advanced DMEM/F12, Gibco, Cat. #11540446)	**Stock**	**Final concentration**
Pen/Strep	100x	1x
HEPES	1 M	10 mM
Glutamax	200 mM	2 mM

Freezing and thawing of PDOs

Patient-derived CRC organoids stored in liquid nitrogen in a cell freezing medium were placed shortly in a 37ºC water bath. Afterward, they were collected and placed into the 15 ml Falcon tube in 5 ml of Basal medium (see *Table 2*). After spinning down organoids at 400 g/1200 rpm and washing them with 1x DPBS, organoids were resuspended with basement membrane matrix drops (30 µL of matrix/well). Next, 30 µL of the BME matrix-organoid suspension was dispensed to the center of wells in a 24-well plate. Approximately 500 µL of WENRAS medium was added to each well, and organoids were incubated at 37ºC and 5% CO2. We performed a medium change every 2-3 days.

For freezing organoids, cryotubes containing freezing medium were thawed and labeled. Media from the well that contains organoids was discarded, and domes were washed with 1x DPBS. Next, we would add a freezing medium to the well. Afterward, we would carefully resuspend the basement membrane matrix containing organoids in the added media. It was essential to perform resuspending step with a precoated pipette tip (Basal growth media + 1% BSA). The suspension was transferred to the prelabeled cryotube and stored in the freezing container at -80°C. After 24h, cryotubes were transferred to liquid nitrogen tanks for long-term storage.

Passaging Patient-derived Colorectal Cancer Organoids

Organoids were passaged when they were too dense and after developing a necrotic core, typically 7-10 days after seeding, ensuring optimal survival conditions. The medium was aspirated entirely from the wells, and TrypLE™ Express Enzyme (1X, Cat. #12605010, Gibco™) + 0.1% Y27632 Rock-inh. was used for organoid digestion. Approximately 500 µL of TrypLE™ was added to the wells, and BME matrix-organoid domes were resuspended with a precoated pipette tip (Basal growth media + 0.1% BSA). Following a short incubation (5-15 min) and disruption of the domes, suspensions were collected in 5 or /15 mL Falcon tubes and centrifuged at 400 g/1200 rpm for 4 minutes. After washing the organoid pellet with 1x DPBS and stopping the digestion, they were resuspended in basement membrane matrix and dispensed to the wells of 12/24-well plates (Buch & Holm A/S).

Organoid lines

Since this project focuses on investigating the epigenetic basis of radio-resistance in rectal cancer, all the performed experiments were mainly focused on using patient-derived organoid line RC1, the only stable rectal organoid line established so far. Due to the lack of other rectal lines, we included the CRC1 organoid line derived from the patient treated with radiotherapy before surgery. Even though we aimed to develop new rectal organoid lines from rectal cancer biopsies, this was unsuccessful due to the quality of the material obtained after the surgery. Therefore, we also included the CRC2 organoid line for the pilot experiments since it was located in the sigma part of the colon and corresponded to the CRC1 (pretreated line). Importantly, this patient did not undergo radiotherapy before surgery.

To conclude, my Master's Thesis project focused on three organoid lines (details shown in *Tables 3* and *4*). All three used organoid lines were previously established by Loan Tran, MSc. During my work, I worked on establishing new lines. However, none of the successful lines was derived from rectal cancer patients. Of course, for the main project's purpose, one of the main aims is to establish a biobank of rectal cancer lines and focus entirely on this tumor entity.

***Table 3**. List of organoid lines included in Master's Thesis Project with enclosed patient's clinical data*

	Age	**Sex**	**Location**	**Diagnosis**	**MSS/MSI**	Treatment
RC1	60	f	rectum	G2, pT3, pN0, L0, V0, R0n/a	MSS	none
CRC1	73	m	sigma	G2, pT2, pN0 (0/19), L0, V0, Pn0	MSS	radiation 25Gy
CRC2	82	f	sigma	G2, pT4a, pN2b (15/19), V0, L1, Pn0	MSS	none

***Table 4**. Driver gene mutations of tumors for included three organoid lines*

	Driver gene mutation (amino acid change)					
	APC	***TP53***	***KRAS***	***FBXW7***	***SMAD4***	***FGFR3***
RC1			G12V	R479Q		
CRC1*	Q1367*	E286G fs*19				
CRC2	T1556N fs*3, V1452S fs*	R342*	G13D	R465H	P356R	F384L

Figure 2 represents brightfield microscope pictures of three included organoid lines.

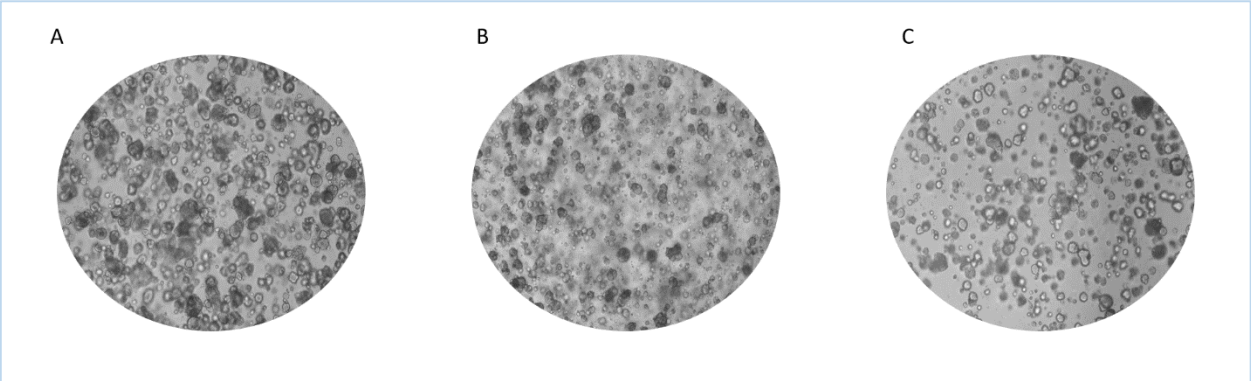

Figure 2. Brightfield microscope images *(scale bar: 500 µM) of RC1 (**A**), CRC1 (**B**) and CRC2 (**C**) organoid lines.*

Using Patient-derived organoids (PDOs) for evaluation of drug response by determination of the half-inhibitory concentration (IC50)

Organoids were digested into single cells using Gibco™ TrypLE™ Express Enzyme. After adding approximately 500 µL of TrypLE™, the Matrigel containing organoids was disrupted using a 1 ml pipette and a pre-coated tip with a coating medium (Basal growth media + 0.1% BSA). Digestion with TrypLE™ followed the same procedure as for passaging organoids except for a longer digestion time since a single-cell suspension was needed. In order to obtain a single-cell suspension, MACS® SmartStrainers were used. The suspensions were transferred to a 15 ml Falcon tube and centrifuged at 400 g/1200 rpm for 4 minutes. The supernatant was aspirated, and the pellet was washed using PBS. Afterward, the pellet was resuspended in 250 µL of 1x DPBS, and the cells were counted using a LUNA™ Automated Cell Counter (Logos Biosystems, Cat. # L10001). Trypan Blue Solution, 0.4% (Gibco™, Cat. # 15250061) and cell solution were mixed in a 1:1 ratio so that 10 µL of each was added and resuspended together. Afterward, 10 µL of final solution was added to the LUNA™ Cell Counting Slides (Logos Biosystems, Cat. # L12002) and placed in the LUNA cell counter. Depending on the number of alive cells/mL, the suspension needed was calculated. Since 105.000 cells are required, this number is divided by the concentration to calculate the required volume of suspension: $required\ volume\ [\mu l] = \frac{105.000}{alive\ cells/\mu l}$. This amount was placed into a 5-ml tube and spinned down. Afterward, the pellet was resuspended in 350 µL of BME matrix. Finally, 10 µL of the suspension was dispensed in the wells of a 96-well plate (Corning®, Cat. #Z713007) and incubated with 90 µL/well of WENRAS medium at 37ºC. With 105.000 cells in total, it is ensured that after seeding 10 µL/well, every well contains 3000 cells. We also included three blank probes (10 µL of BME matrix) that were later important for the read-out.

Following the incubation, Decitabine was added. Serial dilution in WENRAS was prepared *(see Table 5)*, and to every well, 90 µL of each dilution was added. PDOs were treated with 0, 0.05, 0.1, 0.3, 0.5, 1, 3, 5 and 10 µM Decitabine, in triplicates for each concentration (*see Figure 3*).

***Table 5**. DAC serial dilutions preparation (1 sample)*

Dilution	Decitabine (µL)	WENRAS medium (µL)
10 µM	100	900
5 µM	500	500
3 µM	600	400
1 µM	333	667
0.5 µM	500	500
0.3 µM	600	400
0.1 µM	333	667
0.05 µM	500	500
0 µM	/	500

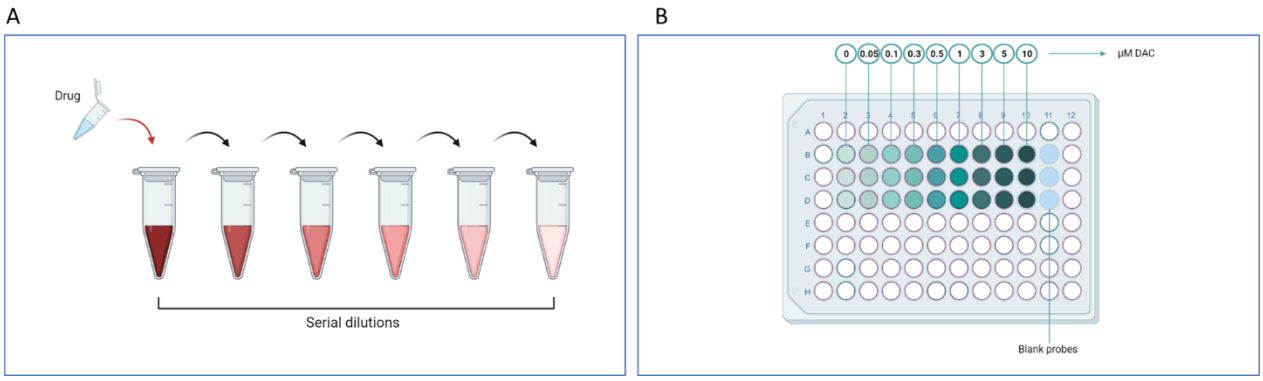

***Figure 3. Drug treatment overview**. **A** – Principle of preparing Decitabine serial dilutions. The calculation used for this protocol is indicated in Table 5. **B** – Decitabine treatment plate representation with the marked layout of the treatments and included blank probes that were important for the read-out.*

The organoids were incubated with the drug for 24h. Afterward, the drug-containing media was replaced with fresh WENRAS medium. Four days after the treatment, the cell viability was measured using CellTiter-Glo® 3D Cell Viability Assay (Promega, Cat. # G9682). The reagent allows the measurement of ATP, which is used as an indicator of viability. To each well, 90 µL of fresh WENRAS medium was added, as well as 100 µL of CellTiter-Glo®. Afterward, the luminescence was measured using a BioTek™ Synergy™ HTX Multi-Mode Microplate Reader. The corresponding Gen5 Data Analysis Software was used for data analysis. The unit for luminescence is RLU (relative light units). From the measured luminescence, the value of blank probes was subtracted. This value (Blank Lum) was plotted on the y-axis of the graphs. The explained procedure is briefly presented on the scheme in *Figure 4*.

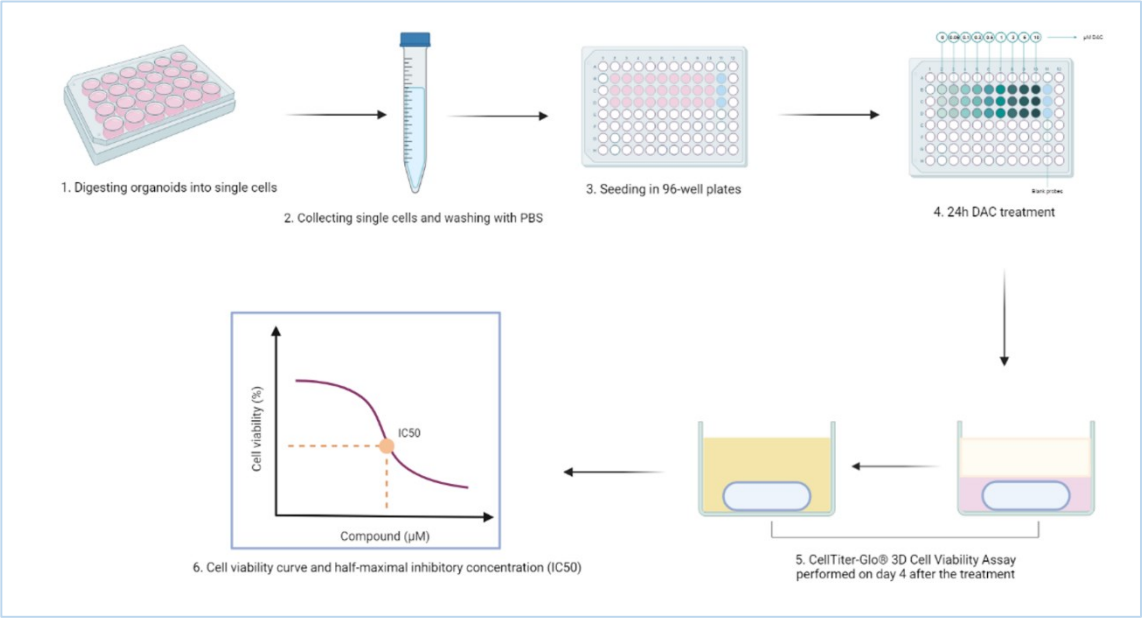

***Figure 4. Graphical summary of the evaluation of drug response with the determination of IC50 value**. After digesting organoids with Gibco™ TrypLE™ Express Enzyme (1), single-cell suspension was collected in 15 mL Falcon tubes and centrifuged. The required volume of single-cell suspension was resuspended in 350 µL BME matrix and seeded in 96-well plates (3). Four days after setting up the experiment, organoids were treated with Decitabine (4). On the fourth day after the treatment, CellTiter-Glo® 3D Cell Viability Assay was performed, and sensitivity curves were obtained (5, 6).*

Using Patient-derived organoids (PDOs) for evaluation of sensitivity towards radiotherapy

As already described in the previous chapter, organoids were digested with TrypLE™ Express Enzyme into single cells, which were counted with LUNA™ Automated Cell Counter. For each condition required to determine radiation response curves, we would seed single cells on different 96-well plates. Our experiments included the following radiation doses: 1, 2, 3, 4, 8, and 12 Gy. Untreated organoids were included as the negative control in every setup. Altogether, we would have five replicates for each of these seven conditions, meaning that 35 domes were seeded for every experiment. Each dome had a volume of 10 µL, and cells were seeded in 300 cells/µL density on 96-well white plates. Similar to DAC treatment experiments, we included blank probes in every plate.

On day 4, organoids were treated with radiation with a YXLON Maxishot X-ray unit. The operation was kindly introduced and carried out at the Department of Radiation Oncology, Medical University of Vienna. We have used the following setting for all irradiation procedures: 200kV 20 mA FOC 5.5. Notably, 0.5 mm Cu + 3 mm Al filters have been used to irradiate the cells. 96-well plates were placed on the PMMA plate, and organoids were irradiated at the dose rate of 1.22 Gy/min. The duration of exposure was applied for radiation doses mentioned above, as stated in *Table 6*.

Table 6. *Radiation dose/time calculation*

Desired radiation dose (Gy)	**Time**	
	Minutes	Seconds
1	0	49
2	1	39
3	2	28
4	3	17
8	6	34
12	9	51

Four days after the radiation treatment, the cell viability was measured using CellTiter-Glo® 3D Cell Viability Assay, as already described in the previous chapter. During the optimization of this experiment, we realized that having different conditions on separate plates is a technical issue when it comes to the read-out. Therefore, we included two concentrations of ATP (Promega, Cat. #P1132) as standards for each of the plates to avoid technical obstacles in the experiment, which allowed us to get a more precise measurement of the luminescence. Finally, we obtained radiation response curves based on the results by using GraphPad Prism 9. From the measured luminescence, the value of blank probes was subtracted. This value (Blank Lum) was plotted on the y-axis of the graphs. The timeline used for these experiments and plate overview can be seen in the *Figure 5*.

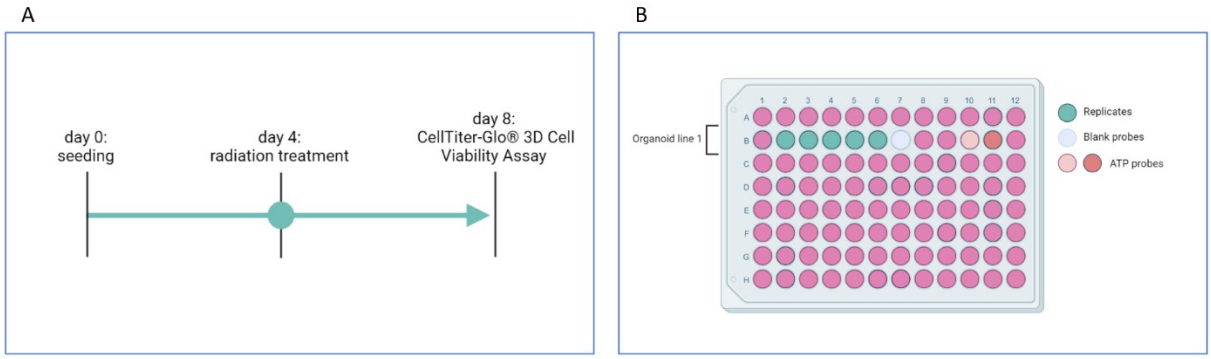

Figure 5. Timeline (A) and plate layout (B) used for evaluation of radiosensitivity*. **A** – For every experiment, organoids were treated with radiation on day 4. On the fourth day after the treatment, we would perform the read-out. **B** – Plate layout indicating that we included five replicates and one blank probe for every condition. Additionally, we included ATP probes to avoid technical obstacles in the experiment.*

Notably, to lower the consumption of CellTiter-Glo® 3D, 96-well plates were used even though only five replicates per condition were needed. To use the capacity of 96-well plates, we either tried to include more organoid lines per experiment or reuse them. However, reusing the plates was not suitable, and organoids seeded in the following experiment would always show certain deviations and difficulties in terms of growth. Therefore, we included more than one organoid line in our set-up whenever possible.

Immunofluorescence

Organoids were seeded in 8-well imaging chambers (ibidi, Cat.#80826) for performing immunofluorescence, with a density of 300 cells/µL. It is important to note that the BME matrix was diluted with 1x DPBS in a ratio of 1:1, which was essential to ensure a faster fixation later. Additionally, when seeding organoids for immunofluorescence, with the help of a pipette tip, we would flatten the domes and spread the 1xPBS/BME matrix drop containing organoids as much as possible over the bottom of the well. It was essential to circumvent touching the chamber walls that would cause issues when changing media afterward.

Two experiments were designed as presented in *Figure 6*. In Experiment 1 (*Figure 6A*), we included four conditions: untreated, DAC treated, radiation treated PDOs, and PDOs treated with the combination of DAC and radiation. Organoids were treated with Decitabine 24h before radiotherapy for the combinational treatment. In Experiment 1, we used yH2A.X and E-cadherin primary antibodies (*see Table 7*). Since we had expected induction of yH2A.X shortly after the radiation treatment, we continued with the immunofluorescence protocol (explained further) on the same day, two hours after the radiation exposure.

We have optimized a setup for Experiment 2 (*Figure 6B*). Firstly, we started with the treatments two days later to make sure that organoids were in better size than the previous experiment. Similarly, we first performed DAC treatment. However, we decided to treat organoids with radiation four days after Decitabine treatment for this setup. We optimized this step to ensure more time for Decitabine to demethylate the genome since we realized that 24h period might be too short. Therefore, radiation was performed on day 10. Finally, since we aimed to observe induction of apoptosis, we have used CC3 primary antibody (*see Table 7*). However, we did not expect a rapid induction of CC3 as for yH2A.X. Therefore, we continued with the immunofluorescence protocol 24h after the irradiation.

Notably, 1 µM Decitabine and 2Gy radiation were used in these experiments.

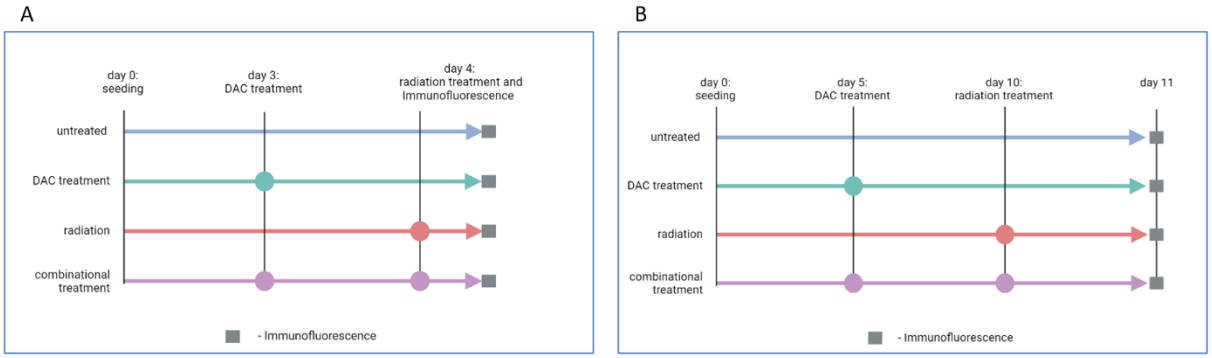

***Figure 6. Timeline for Immunofluorescence Experiment 1 (A) and 2 (B). A** – We seeded all four conditions on the same day. DAC- and combination-treated organoids were treated with Decitabine on day 3. Radiation- and combination-treated organoids were irradiated on the following day. On the same day, we continued with immunofluorescence protocol. **B** – Unlike the previous experiment, DAC treatment was performed on day 5. Five days later, we irradiated the organoids and continued further with the experiment on the next day.*

Before starting with the immunofluorescence protocol, we prepared all the necessary buffers needed for the experiment (*see Table 8*). To begin with, we washed BME matrix domes containing organoids 2x with 1x DPBS. To each well, 150 µL of Fixation solution was added. Chamber slides were then incubated for 30 minutes at room temperature (RT), ideally on the rocking platform. Next, wells were washed three times with 1x DPBS. Afterward, 150 µL of permeabilization buffer was added, and chamber slides were again incubated for 30 minutes at RT. Further, we added fresh blocking buffer to the wells after being washed three times with 1x DPBS. Finally, after 30 minutes of incubation, freshly prepared primary antibodies (diluted in blocking buffer) were added *(see Table 7*), and chambers were left overnight at the rocking platform (4ºC).

On the following day, wells were washed three times with the washing buffer, and a freshly prepared secondary antibody (diluted in the blocking buffer) was added. Chamber slides were incubated for two hours and then washed again. Finally, DAPI (1 µg/mL) was added to the wells.

After the final incubation of 20 minutes, wells were washed once and mounted with the mounting medium (ibidi, Cat. # 50001).

***Table 7**. List of antibodies used for Immunofluorescence*

Target	Type	Organism	Provider	Dilution
E-cadherin	primary	mouse monoclonal	*ab1416 Abcam*	1:150
CC3	primary	rabbit polyclonal	*9661 Cell Signaling*	1:400
yH2A.X	primary	rabbit polyclonal	*STJ97185 Clementia Biotech*	1:100
Alexa Fluor 488	secondary	goat anti-rabbit	*A-11034 Invitrogen*	1:1000
Alexa Fluor 594	secondary	goat anti-mouse	*A-11005 Invitrogen*	1:1000

***Table 8**. Immunofluorescence solutions and buffers*

Solution	Component	Stock concentration	Final concentration
Fixation solution	PFA	-	4 %
	PBS	-	1x
Washing buffer	PBS	-	1x
	Triton-X 100	10 %	0,1 %
	Tween	10 %	0,05 %
Permeabilization buffer	PBS	-	1x
	Triton-X 100	10 %	0,5 %
Blocking buffer	PBS	-	1x
	Triton-X 100	10 %	0,1 %
	Goat serum	100 %	10 %

Embedding Organoids for Immunohistochemistry (IHC)

This protocol was established by Tanja Limberger, written by Jessica Kalla, adapted, and provided by Theresia Mair.

Organoids were seeded in a BME matrix (300 cells/µL). We would keep them in culture for several days before starting with embedding. This period differs among organoid lines since they may show diverse growth rates. However, after seven days, most organoid lines were already ready for embedding.

Domes of BME matrix containing organoids were washed two times with 500 µL 1x DPBS. Afterward, 4.5% formaldehyde (PFA) was added and incubated for 15 minutes at room temperature. Further, organoids were resuspended and then fixed for additional 15 minutes. After the incubation time, organoids were transferred to the precoated 5 mL Eppendorf tube. When resuspending/transferring organoids, it was crucial to precoat the tip with 0.1%BSA/DPBS to avoid organoids sticking to the tip. To collect the organoids in the bottom of the tube, we centrifuged tubes for 5 minutes at 300 g. Following two washing steps (with 1 ml 0.1%BSA/DPBS), 50 µL of Eosin was added, and organoids were incubated for 10 minutes at RT. Afterward, washing organoids several times with 0.1%BSA/DPBS ensured that only organoids

remained stained with Eosin. Finally, organoids were resuspended in 1% agarose with a precoated tip and pipetted into the hole in the prepared silicone mat. The last step was performed in a preheated water bath and with preheated and precoated tips, which ensured that agarose did not solidify during the process. After 30 minutes of incubation on ice, agarose domes were transferred on cassette insert paper and placed in histology cassettes. Cassettes were placed into 4.5% PFA for 15 minutes and then moved to 70% EtOH.

The following step was dehydration of the agarose domes, performed routinely at the Clinical Institute of Pathology of Vienna General Hospital. Finally, agarose domes were embedded into paraffin.

Further steps of cutting and staining were performed and kindly provided by Sabrina Wohlhaupter. Finally, IHC slides were scanned using The PANNORAMIC 250 Flash Slide Scanner and analyzed using CaseViewer.

Harvesting Patient-derived Organoids

After discarding medium from wells that contained organoids that needed to be harvested, domes were washed 3x with 1x DPBS. Next, organoids in the BME matrix were resuspended with Cell Recovery Solution (Corning®, Cat. #354253). For each well of 24-well plate, we used 1-2 mL of the solution. This suspension was then transferred to a 5- or 15-mL Falcon tube and placed on ice. The samples were incubated for 30-60 minutes on a rocking platform (80-90 rpm). When pelleted, organoids were washed once with 1x DPBS, ensuring that all organoids that remained sticking to the wall were pelleted. After centrifugation (5 minutes, 400 g/1200 rpm), 1x DPBS was removed, and tubes were snap-frozen in liquid N2. They were stored at -80°C until needed for further processing.

In case single cells were needed (usually in experiments that required a certain number of cells), organoids were first digested with TrypLE™ Express Enzyme. After counting, a certain amount of the single cells was snap-frozen in liquid N2.

Extraction of DNA from Patient-derived Organoids

DNA was isolated according to QIAGEN QIAamp® DNA Mini Kit with some adjustments. Instead of performing steps 1-3 as explained in protocol, snap-frozen organoid/cell pellets were resuspended in 200 µl PBS, 200 µl Buffer AL and 20 µl Proteinase K. This was incubated 30 minutes at 56°C on the Eppendorf ThermoMixer. Then, steps 4-8 were performed as explained in the protocol. For step 9 (elution step), 60 µl of New England BioLabs® Inc. Nuclease-free Water (#B1500S) was used.

The DNA concentration was measured using Qubit dsDNA HS (High Sensitivity) and Qubit dsDNA BR (Broad Range) assay kits.

Bisulfite conversion

For DNA bisulfite conversion, we used EZ DNA Methylation™ Kit (Zymo Research, Cat. #D5002), and we followed the entire procedure explained in the provided protocol. We would always add 1 µg of input DNA. In the last step, we would elute DNA in 200 µL of New England BioLabs® Inc. Nuclease-free Water. Even though it is impossible to measure the DNA concentration after the bisulfite conversion, by eluting 1 µg of DNA in 200 µL of Nuclease-free Water, we made sure to have the concentration of approximately 5ng/µL.

If the DNA concentration measured after DNA isolation was too low for adding 1 µg of DNA input, we would add 500 ng of DNA and elute it in 100 µL instead. This would secure the same final concentration of converted DNA.

We also included DNA from Human Methylated & Non-Methylated (WGA) DNA Set (Zymo Research, Cat. #D5013). Bisulfite-converted methylated and non-methylated DNA were used as controls for the reaction success. Additionally, methylated WGA DNA was diluted either in water or non-methylated DNA, as explained further in the following chapter. These dilution series were used as standards for MethyLight experiments.

MethyLight

Converted DNA was further used to evaluate the LINE1 methylation level through MethyLight experiments. Firstly, we would prepare all dilutions required. For these experiments, we included two sets of standards. We used standards 1-5 to check primer efficacy and how well our primers can recognize still fully methylated but diluted DNA. To prepare these standards, fully methylated WGA DNA was diluted in nuclease-free water, as shown in *Table 9*.

***Table 9**. Preparation of Standards 1-5, used for determination of primer efficacy*

Standards 1-5	**DNA (ng/µL)**	**Volume added (µL)**	
		Methylated DNA	**Nuclease-free Water**
ST1	5	20	/
ST2	0.5	2	18
ST3	0.05	2	18
ST4	0.005	2	18
ST5	0.0005	2	18

Furthermore, we included Standards I-V to check for primer specificity. In other words, this was important in showing us how well our primers can distinguish the methylated DNA from non-methylated DNA. The calculation for the preparation of these standards is indicated in *Table 10*.

***Table 10**. Preparation of Standards I-V, used for determination of primer specificity*

Standards I-V	% Methylation	Volume of DNA added (µL)	
		Methylated	Non-methylated
I	100	20	/
II	10	2	18
III	1	2	18
IV	0.1	2	18
V	0	/	20

In our MethyLight experiment, we included two different sets of primers. We used the ALU methylation level as a normalization control that would help us estimate the amount of DNA added to each well. On the other hand, we used LINE1 methylation to study global DNA methylation level changes. For each of these, we prepared separate Oligo Mix, as indicated below in *Table 11*.

***Table 11**. Oligo Mix preparation*

	Stock (µM)	Final (µM)	Volume (µL)
Forward primer	100	2	6
Reverse primer	100	2	6
Probe	100	0.67	2
Nuclease-free water			286
Oligo Mix Solution			**300**

Every Oligo Mix was kept at -20ºC and thawed whenever needed. Furthermore, we prepared Master Mix for ALU and LINE, as indicated in *Table 12*. Importantly, Master Mix was prepared freshly for every experiment, as shown below. *Table 12* suggests a calculation used for one sample. We would multiply the indicated volumes with the number of wells needed for the experiment, considering 10% of possible error for the final count.

***Table 12.** Master Mix preparation (1x)*

	Volume (µL)
Oligo Mix	2.25
TaqMan Universal PCR Mix	7.5
Nuclease-free water	3.25
Master Mix Solution	**13**

Finally, we would pipette the reaction. Below are indicated volumes of DNA and Master -Mix that were added to a white Multiplate™ 96-Well PCR Plates (Biorad, Cat. # MLL9651):

- 13 µL Master Mix
- 2 µL DNA

We included each sample in triplicates for both ALU and LINE1 Master Mix. On the other hand, standards were screened only for ALU elements methylation.

For running the MethyLight experiment, we used the protocol stated below, which was run on C1000 Touch Real-Time Thermal Cycler CFX96 (Biorad).

1. 1 cycle at 95ºC (10 min)
2. 50 cycles at 96ºC (15 sec)
3. 50 cycles at 60ºC (1 min)
4. Step for capturing melting curves

Finally, we would calculate the PMR (%) based on the Excel template provided by Loan Tran, MSc and generated based on the protocol for MethyLight in DNA Methylation Methods (chapter 23) [37]. For the PMR (%) calculation, we used the following formula:

$$PMR(\%) = \frac{Sq\ ratio\ (\frac{LINE1\_sample}{Alu\_sample})}{Sq\ ratio\ (\frac{LINE1\_\ 100\%methylated\ control}{Alu\_\ 100\%\ methylated\ control})} \times 100$$

Evaluation of the effect of single and combinational treatments on DNA methylation

As previously explained, parts 1 and 2 of the project aim to investigate the potential effect of radiation treatment and combinational treatment on DNA methylation. To tackle this, we performed the pilot experiment to compare the outcome of low-dose single treatments (radiotherapy/DAC treatment) and combinational therapy and having untreated organoids as the control. Outline of the experimental setup can be seen in *Figure 7*. RC1 organoids were digested into single cells, counted with LUNA automated cell counter, and seeded in 12-well plates. On day 4, organoids were treated with 0.5 µM DAC. This drug concentration was used since a low dose of both treatments was needed. IC50 of this line is ~ 3 µM (see Decitabine drug treatments and determination of IC50 values), and 0.5 µM was selected as the desired low dose, which is ~20% of its IC50 value. Untreated and DAC treated organoids were harvested on day 8. Other organoids were treated with low-dose radiation therapy (1Gy) on the same day. Like the low DAC dose, a low radiation dose was determined based on the radiation response curves obtained beforehand (see Radiation response curves). The remaining organoids were harvested on day 12. We performed all harvesting steps based on the protocol explained in the paragraph Harvesting organoids.

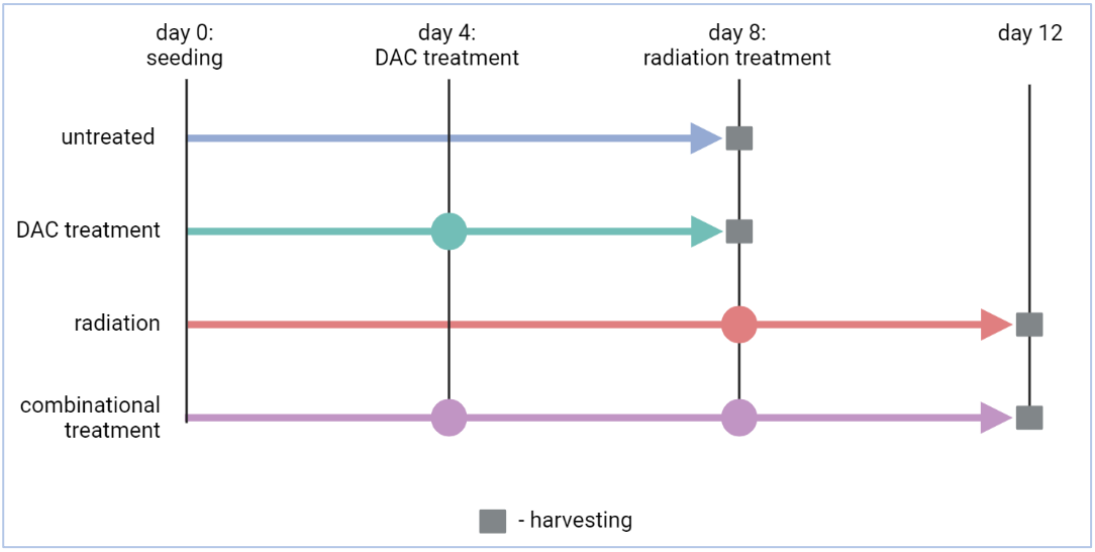

Figure 7. Timeline used for evaluation of the effect of treatments on DNA methylation. *On day 4, DAC- and combination- treated organoids were treated with 0.5 µM DAC. Four days after, radiation- and combination-treated organoids were irradiated. Harvesting was done on days 8 and 12, as indicated in the Figure.*

DNA isolation was performed as previously described in DNA extraction from organoids when all samples were collected. Then, we sent DNA samples for Illumina Infinium® Methylation EPIC array. Additionally, we used the remaining DNA to evaluate LINE1 methylation levels among different treatment conditions.

Timepoint Determination

To investigate whether there is a specific time point in which changes in global DNA methylation upon radiation treatment can be observed, 'Timepoint Determination' experiments were performed. As shown in *Figure 8*, we included three different conditions in these experiments for every organoid line: untreated organoids, as well as 1Gy- and 12Gy-treated organoids. The main goal was to investigate the possible effect of low-dose and high-dose treatment on global DNA methylation. Additionally, different harvesting time points were essential to determine when this potential effect might be happening.

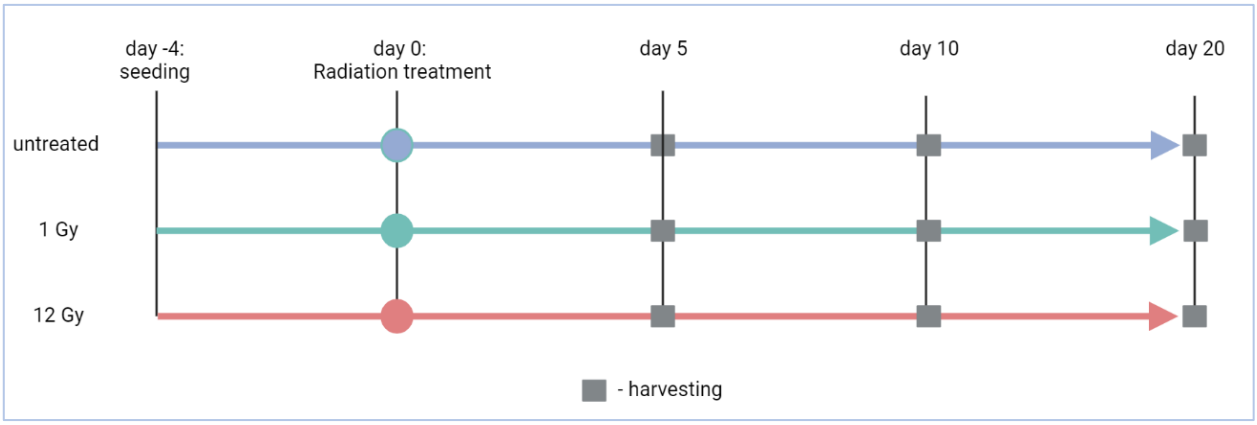

Figure 8. Timeline used for timepoint determination experiments*. All organoids were seeded and treated on the same day. Harvesting was performed on days 5, 10, and 20.*

On the day of seeding (day -4), organoids were digested into single cells and counted with LUNA automated cell counter. Single cells were seeded on three plates, each for different treatment conditions. On day -4, cells were seeded in 8 domes per condition, with a density of 500 cells/µL. Each dome had a volume of 30 µL and 15.000 cells in total.

Harvesting of cells was performed on days 5, 10, and 20. Organoids were again digested into single cells and counted. Counting provided valuable information about the percentage and number of live cells after different treatments. Most single cells were snap-frozen in liquid nitrogen and stocked for further processing. A small portion of cells was reseeded for the subsequent harvesting in the same density used on day -4. Even though day 20 was defined as the last time point, reseeding of single cells was performed on that day as a backup for possible further analysis.

Snap-frozen cells were further used for DNA isolation (see *), bisulfite sequencing (see *), and analysis of LINE1 methylation levels by performing MethyLight experiments (see *). We used LINE1 methylation level to estimate the level of global DNA methylation and its changes upon radiation treatment at different time points.

Results

Comparing the rate of PDOs growth in different BME matrices

We performed several experiments to evaluate the success rate of growing our organoid lines in different Basement Membrane Extract (BME) matrices. Firstly, the cell viability of organoids grown in different matrices in the same period was measured using CellTiter-Glo® 3D Cell Viability Assay. Then, data were further analyzed by using GraphPad Prism. Since the same number of single cells was seeded on the same day but in different conditions, these results provided valuable information about how our organoid lines grow in various BME conditions. Therefore, we could conclude which BME matrix is the most favorable based on the GraphPad Prism bar graphs (*see Figure 9*) and evaluated significance by One-way ANOVA and Turkey's Multiple Comparisons Analysis. Our results indicated that cell viability of all tested organoid lines was higher when grown in Corning® Matrigel® Matrix compared to other tested extracellular matrices. *Figure 9A* shows that there was a significant difference compared to Gibco™ Geltrex™, Cultrex Organoid Qualified BME, Type R1, and Type 2 in the growth of line CRC1. However, there was no significant difference between different conditions in the growth of CRC2 (*see Figure 9B*).

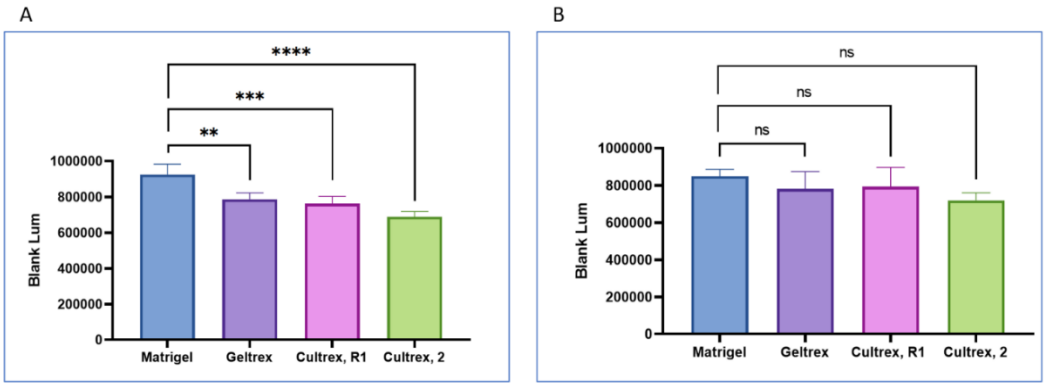

Figure 9. Cell viability of organoid lines CRC1 (A) and CRC2 (B) in different BME matrices. *A – Cell viability of CRC1 organoids measured by Cell titer glow 3D assays for organoids grown for 7 days in Corning® Matrigel® Matrix (Matrigel) compared to Gibco™ Geltrex™ , Cultrex Organoid Qualified BME, Type R1, and Type 2 .* ***B*** *–Cell viability of CRC2 organoids grown in different BME matrices as in (A). ns, not significant, **P < 0.005, ***P < 0.001, ****P <0.0001. Statistical significance was determined by Ordinary one-way ANOVA and Turkey's Multiple Comparisons Analysis of raw data. Standard deviation between technical triplicates is indicated in the chart.*

When analyzing the microscopic figures of CRC1 taken at different time points (*see Figure 10*), one can appreciate that this line is highly proliferative when growing in Corning® Matrigel® Matrix. On the other hand, this line seems to be growing slowest when cultured in Cultrex Organoid Qualified BME, Type 2. In *Figure 11,* microscopic images are shown, going along with the results obtained from the previously explained analysis and the results shown in *Figure 9B*. Even though there was no significant difference among several conditions, the CRC2 organoids grew denser when using Corning® Matrigel® Matrix. Importantly, these images were not quantified.

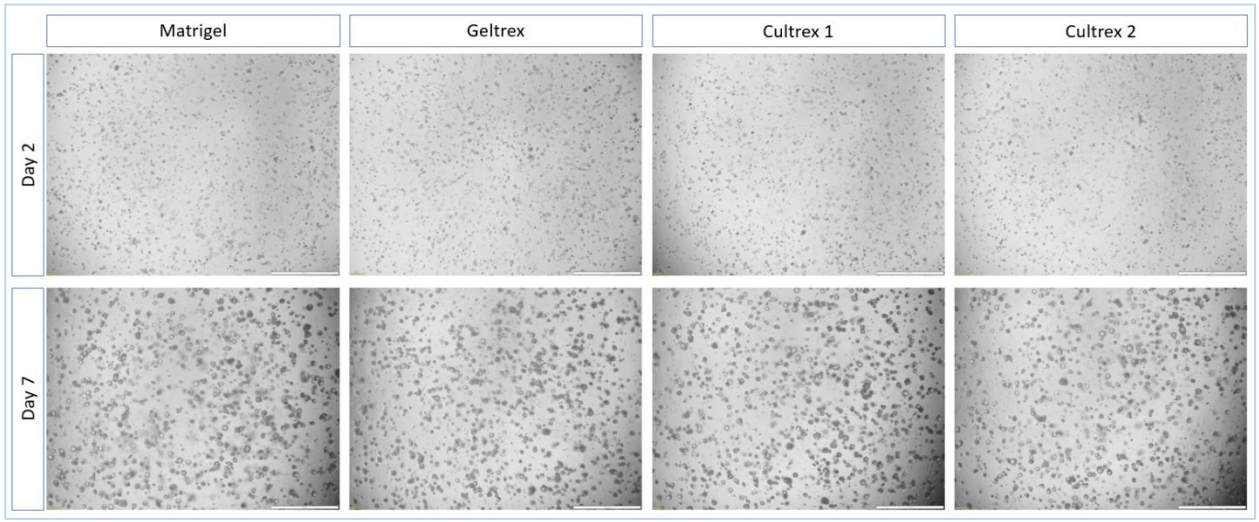

Figure 10. Brightfield images (scale bar: 500 µM) of CRC1 showing the growth of organoids in different BME matrices. *Brightfield images of CRC1 organoids grown in different BME matrices were taken on two different time points (day 2 and day 7) in order to track their growth and density.*

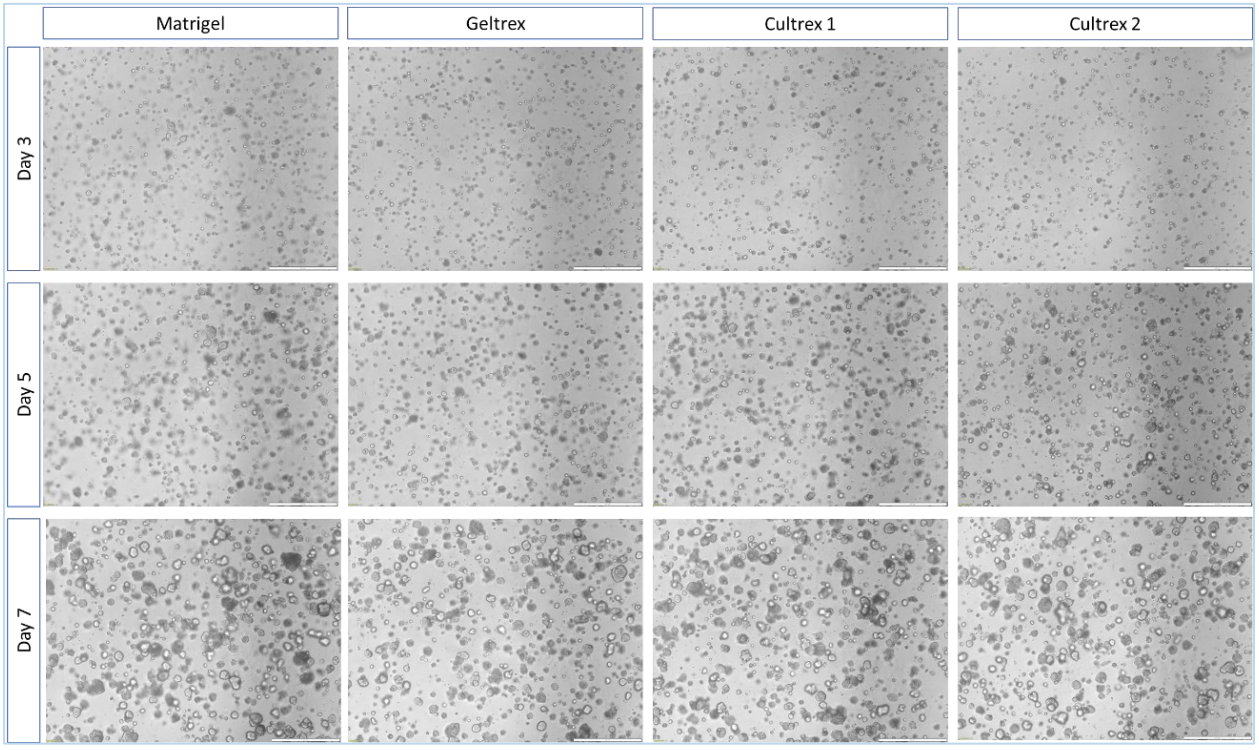

Figure 11. Brightfield images (scale bar: 500 µM) of CRC2 showing the growth of organoids in different BME matrices. *Brightfield images of CRC2 organoids grown in different BME matrices were taken on two different time points (days 3, 5 and 7) in order to track their growth and density.*

Finally, to further explore the microanatomy and proliferation of our organoid lines, we performed histo-morphological analyses using hematoxylin and eosin (H&E) staining and immunohistochemistry for the proliferation marker Ki67. However, since we did not observe any significant difference, this data is not shown.

Decitabine drug treatments and determination of IC50 values

To determine IC50 values of Decitabine (DAC) among our organoid lines and to investigate whether the lines we used were sensitive or resistant towards this DNMTi, we evaluated the drug response of different organoid lines by determination of the half-inhibitory concentration (IC50). The representative graphs for lines RC1, CRC1, and CRC2 are shown in *Figures 12-14*, respectively.

Based on these results, we conclude that IC50 of RC1 = ~ 3 µM; CRC1 = > 10 µM; and CRC2 = ~ 4 µM. In regards to other organoid lines, screened as the part of the Loan Tran's PhD project, where IC50 dose for median sensitive lines was shown to be between 1 and 2 µM, they were found to be rather resistant.

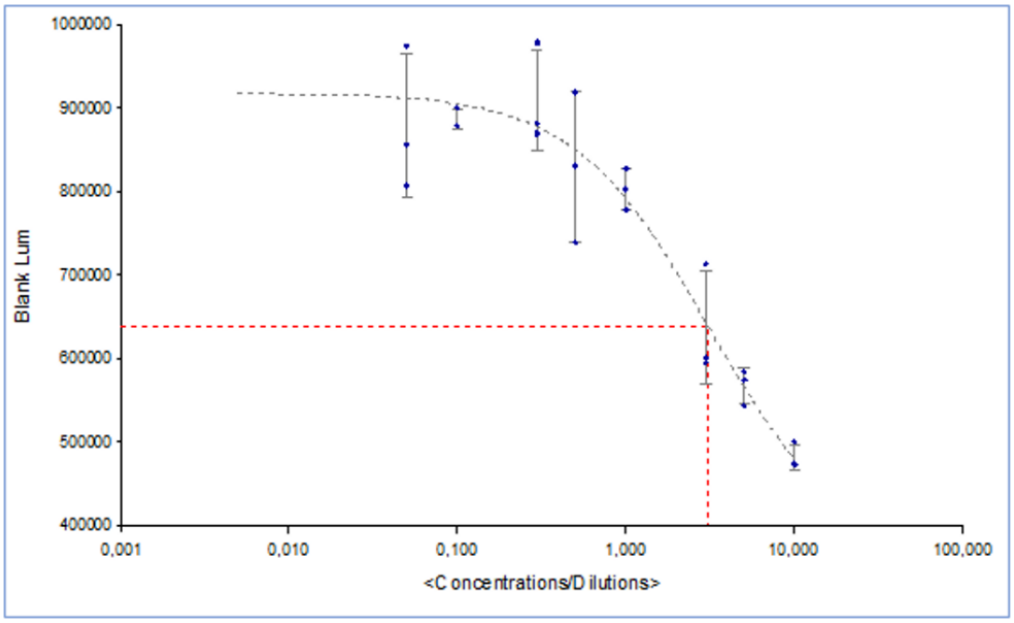

Figure 12. Representative IC50 graph for RC1 organoid line. *The IC50 value and fitting curve, calculated automatically by the Gen5 Data Analysis Software, are represented in the chart. Concentrations (log) are plotted on the x-axis, while the luminescence subtracted for the blank probe value is plotted on the y-axis. Standard deviations between technical triplicates are also indicated in the chart.*

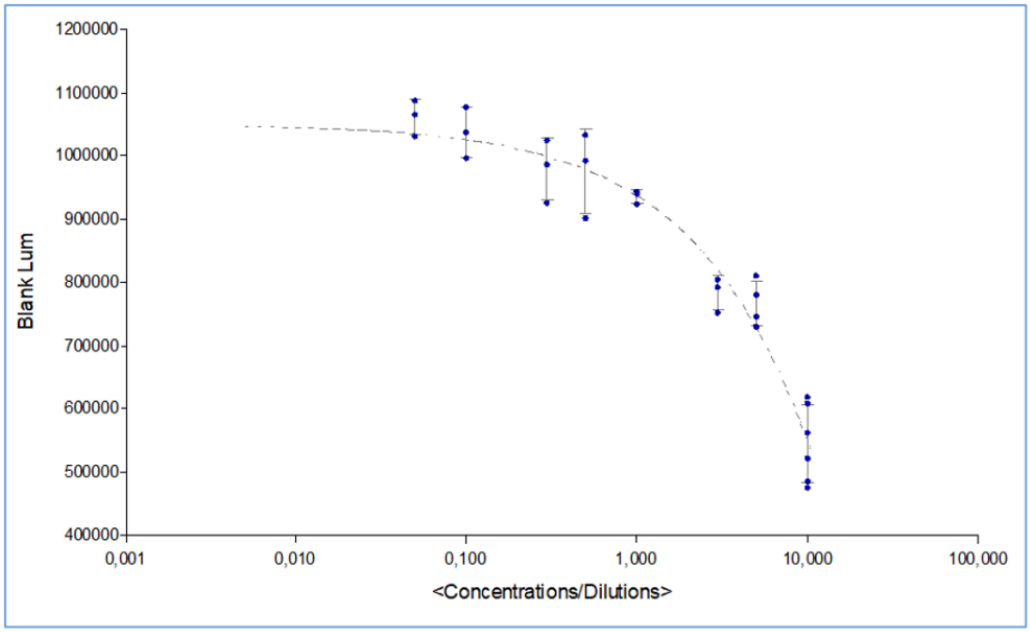

Figure 13. Representative IC50 graph for CRC1 organoid line. *The fitting curve, calculated automatically by the Gen5 Data Analysis Software, is represented in the chart. Concentrations (log) are plotted on the x-axis, while the luminescence subtracted for the blank probe value is plotted on the y-axis. Standard deviations between technical triplicates are also indicated in the chart.*

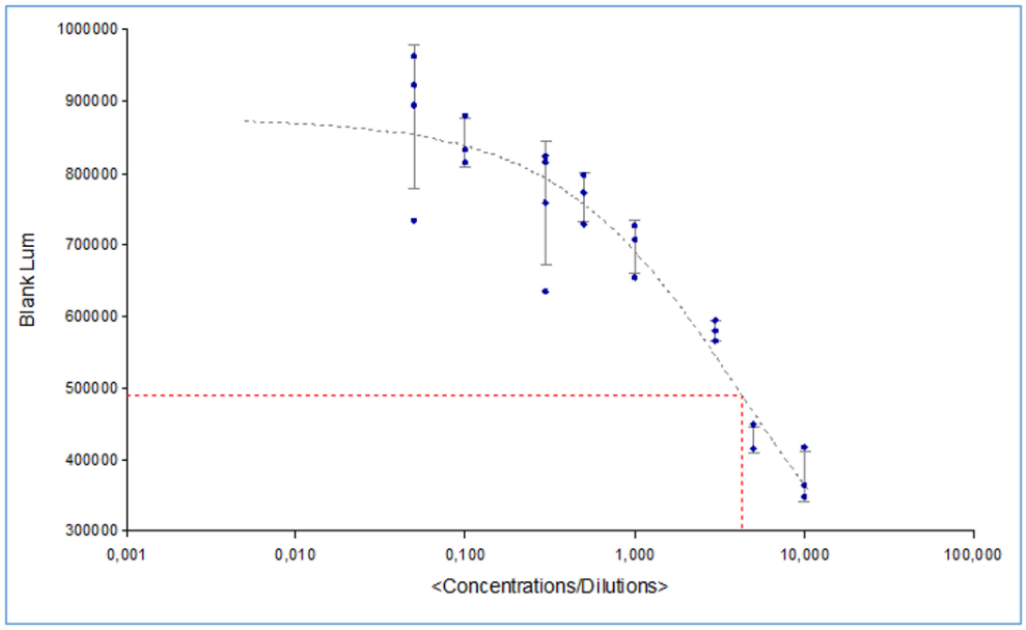

Figure 14. Representative IC50 graph for CRC2 organoid line. *The IC50 value and fitting curve, calculated automatically by the Gen5 Data Analysis Software, are represented in the chart. Concentrations (log) are plotted on the x-axis, while the luminescence subtracted for the blank probe value is plotted on the y-axis. Standard deviations between technical triplicates are also indicated in the chart.*

Radiation response curves

To estimate the sensitivity of our PDO lines towards radiotherapy, we performed a dose response measurement using increasing radiation of 1, 2, 3, 4, 8, and 12 Gy . *Figure 15* shows representative radiation sensitivity curves derived for RC1 and CRC2 lines.

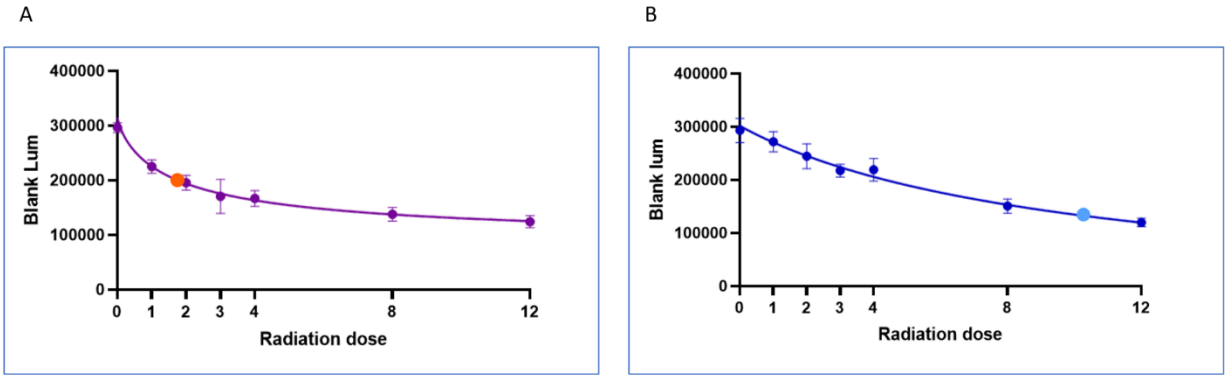

Figure 15. Radiation response curves of RC1 (A) and CRC2 (B). *Generated response curves and doses of half-decreased luminescence marked with orange and light-blue circles for RC1 (A) and CRC2 (B), respectively, are shown in the Figure. The Curve Fitting with Nonlinear Regression was generated using GraphPad Prism (the used equation: "[Inhibitor] vs. response -- Variable slope – four parameters"). In both A and B, luminescence subtracted for the blank probe value was plotted on the y-axis. The unit for luminescence is RLU (relative light units). Standard deviations between technical triplicates are also indicated in the chart.*

As shown in *Figure 15*, based on the sensitivity curves and values calculated as doses that lead to half-decreased luminescence four days after the radiation, we could conclude that RC1 is more sensitive compared to CRC2. Based on the obtained results, we have defined high- and low-doses necessary for all further experiments requiring a certain level of radiation as part of the set-up.

Furthermore, brightfield images taken on days 0, 4, and 8 and shown in *Figures 16* and *17* indicate different responses towards radiation. The effect of the treatment was more prominent in the RC1 organoid line. Importantly, even though untreated CRC2 organoids seem to be denser than RC1, a similar level of luminescence (*see Figure 15*) indicates the approximately same level of cell viability of untreated organoids for both lines. Importantly, brightfield images were not quantified. However, based on these results, we conclude that we identified a radiosensitive (RC1) and radioresistant (CRC2) organoid line.

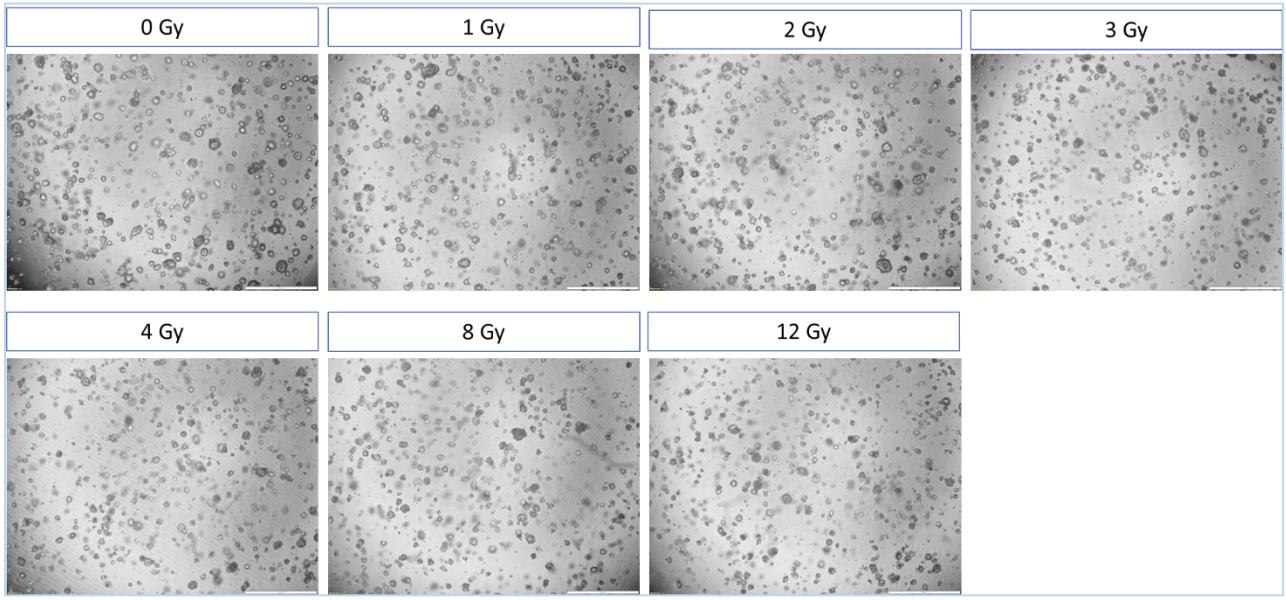

Figure 16. Brightfield images (scale bar: 500 µM) of RC1 on day four after the radiation treatment. *Brightfield images of the RC1 organoid line treated with different doses of radiotherapy were taken on day four after the irradiation. These images were used for further validation of the radiation response curve. The pictures were not quantified.*

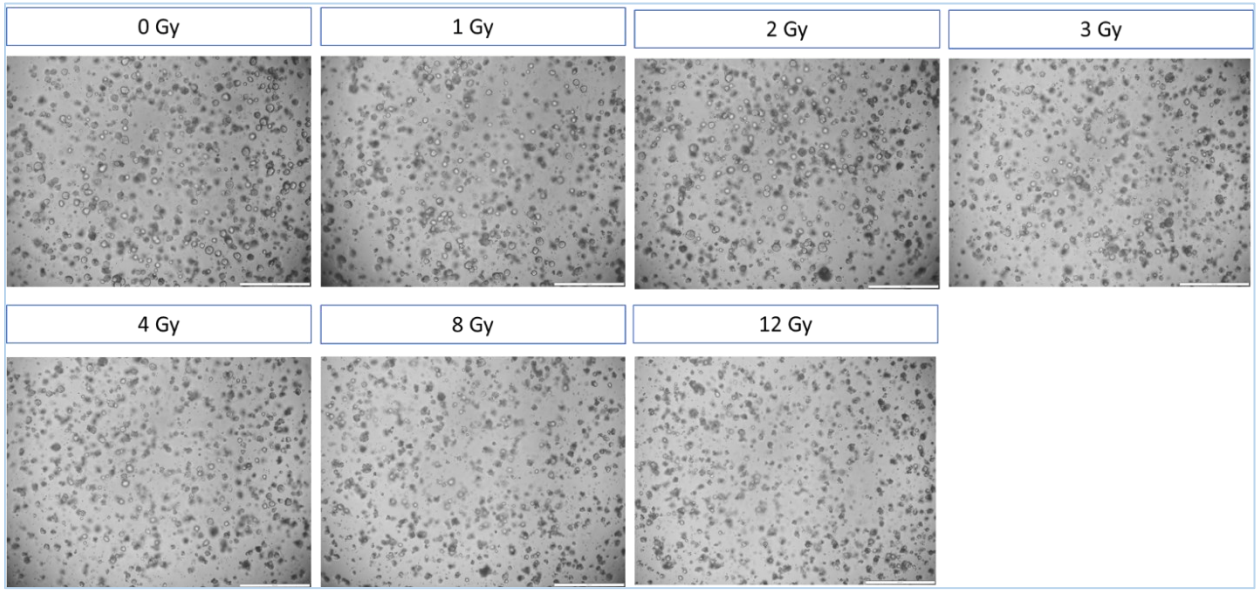

Figure 17. Brightfield images (scale bar: 500 µM) of CRC2 on day four after the radiation treatment*. Brightfield images of the CRC2 organoid line treated with different doses of radiotherapy were taken on day four after the irradiation. These images were used for further validation of the radiation response curve. The pictures were not quantified.*

The same experiment was performed for the CRC1 organoid line. The radiation response curve obtained for this line is shown in *Figure 18*. It suggests that CRC1 is rather radioresistant organoid line compared to other tested lines. However, due to the high standard deviation between technical triplicates, and rather low level of luminescence compared to other organoid lines, this has to be further validated.

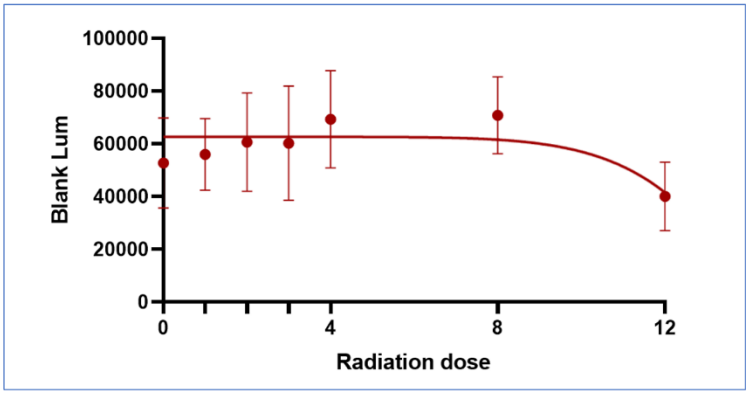

Figure 18. The radiation response curve of CRC1. *Generated radiation response curve for CRC1 organoid line is represented. The Curve Fitting with Nonlinear Regression was generated using GraphPad Prism (the used equation: "[Inhibitor] vs. response -- Variable slope – four parameters"). The luminescence subtracted for the blank probe value was plotted on the y-axis, while radiation dose was plotted on the x-axis. Standard deviations between technical triplicates are also indicated in the chart.*

Comparing the effect of single- (Decitabine/radiation) or combination-treatment on organoids by performing immunofluorescence experiments

To analyze the effects of single or combination treatments of DNMTi and radiation on DNA damage we performed immunofluorescence staining for γH2A.X. Images shown in *Figure 19* show representative organoids and indicate no effect of the pretreatment with DAC on the induction of γH2A.X in organoids treated with combinational treatment. We detected increased levels of γH2A.X in organoids treated with DAC and radiation compared to untreated organoids. No significant changes were observed between radiated or combination-treated organoids.

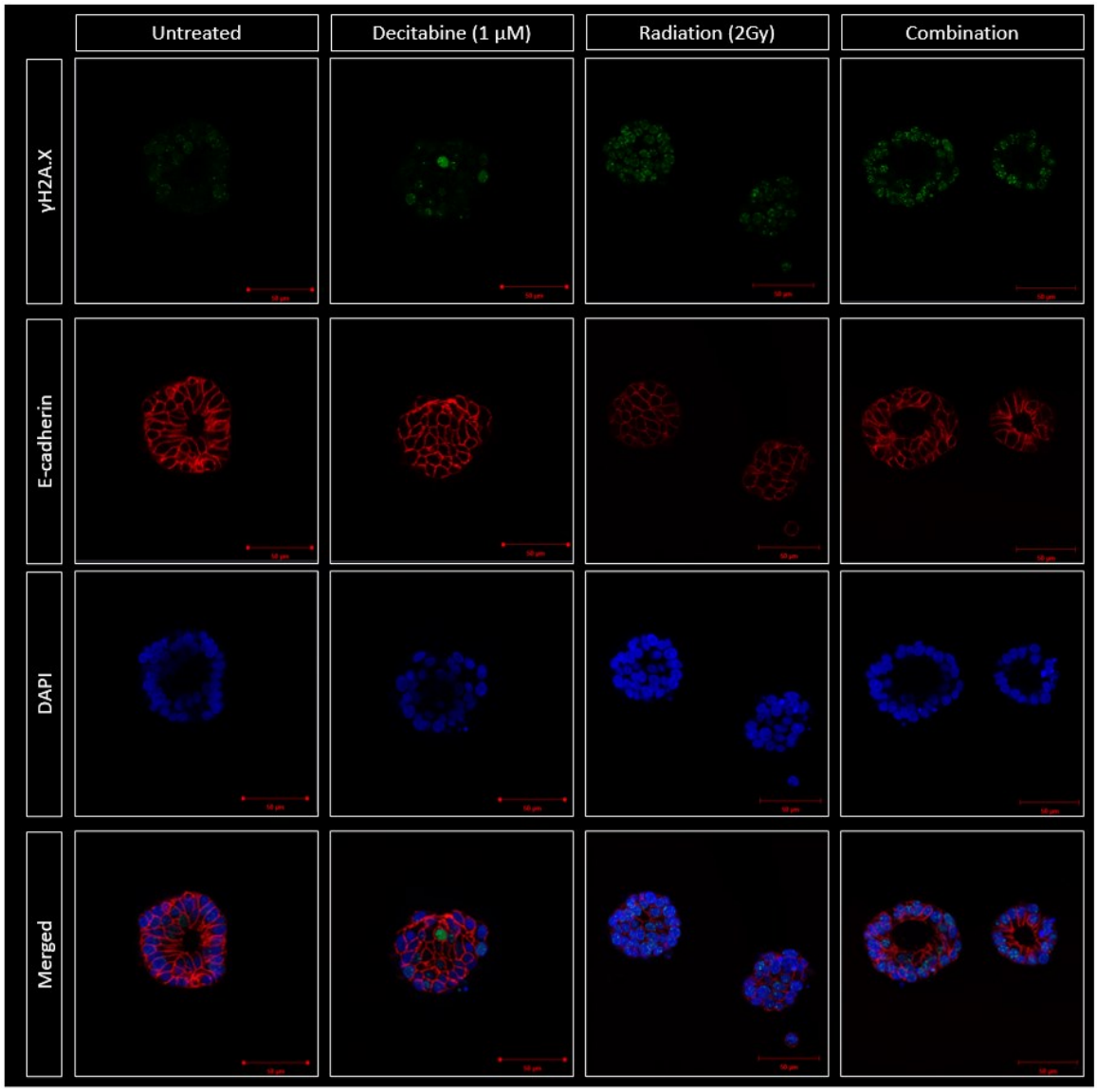

Figure 19. Immunofluorescence figures of RC1 organoid line treated with Decitabine/radiation/combination therapy and stained for γH2A.X. *Immunofluorescence images of organoids treated with different treatments and stained for the γH2A.X marker are shown in this Figure. These are representative pictures that show the effect of single- and combination-treatments on the level of DNA damage (scale bar: 50 µM).*

In the second experiment, we analyzed the induction of apoptosis using caspase3 as a marker. As seen from *Figure 20,* in the case of RC1, we did not observe any effect of the DAC pretreatment on the response to radiation. However, we observed a strong induction of CC3 in CRC1 organoids that were pretreated with DAC prior to radiation, compared to radiation-only treatment. Importantly, as shown in the previous chapter, CRC1 organoid line seems to be highly resistant to radiation. Therefore, these results may indicate a possible benefit of pretreating resistant organoids with DAC before irradiation.

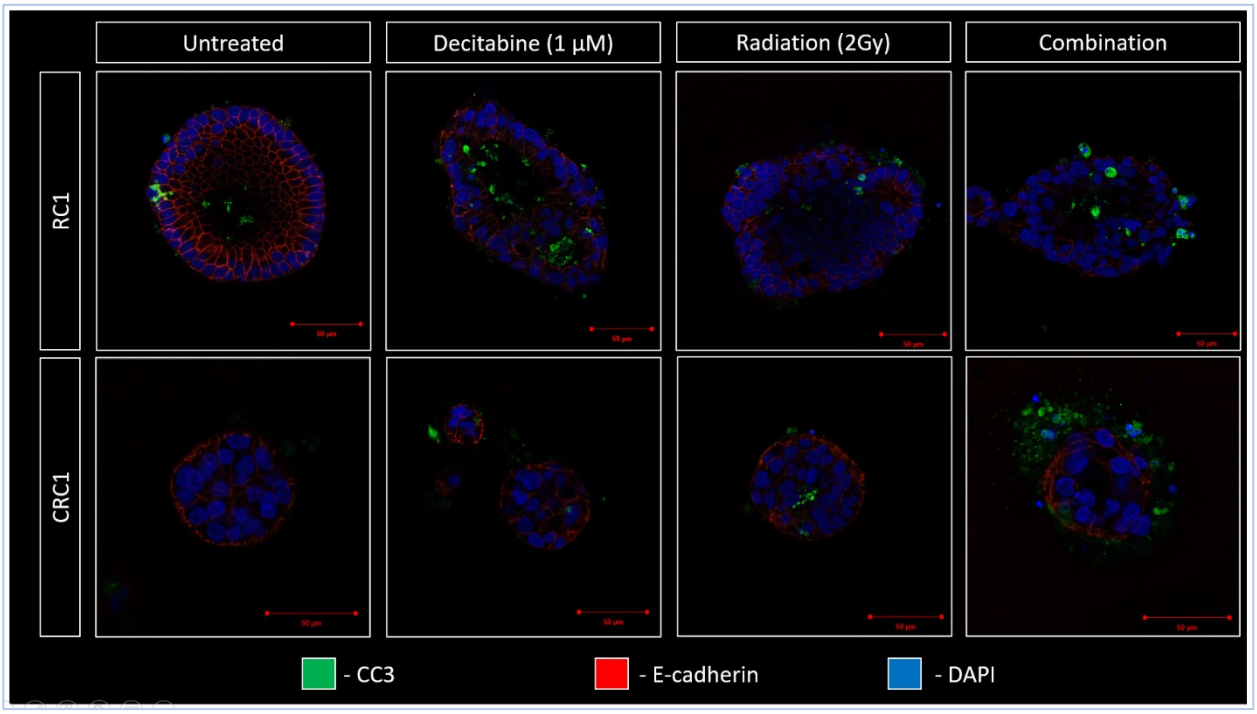

Figure 20. Evaluation of possible benefit of DAC-pretreatment on the radiation response*. These are representative immunofluorescence pictures that show the effect of single- and combination-treatments on the CC3 induction (scale bar: 50 µM).*

Exploring the effect of radiotherapy on global DNA methylation level

In order to study a potential effect of radiation on global DNA methylation levels, we analyzed the effect of different treatments on LINE1 methylation level.

Statistical analysis by Ordinary one-way ANOVA and Turkey's Multiple Comparisons Analysis indicated no significant changes in LINE1 methylation level between untreated and radiated organoids (*Figure 21)*. Furthermore, DAC treated organoids showed about 50% reduction of DNA methylation, which was similar to the methylation levels of organoids treated with radiation after the DAC treatment, indicating no further effect of radiotherapy on the LINE1 methylation level. Notably, the LINE1 methylation level of untreated organoids remained the same even after two passaging steps, indicating DNA methylation stability in our organoid cultures.

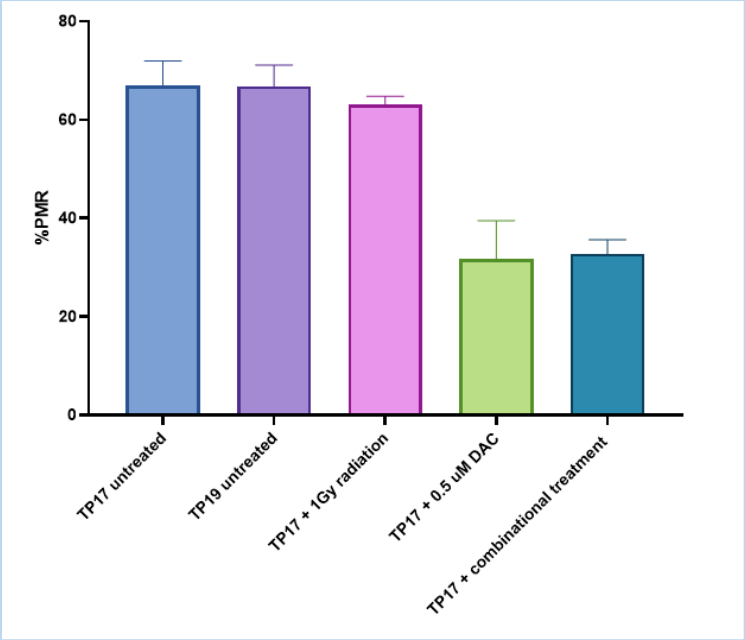

Figure 21. Changes of LINE1 methylation level upon single radiation/DAC treatment and combination (radiation + DAC) treatment. *Besides expected effect of DAC treatment, we wanted to further evaluate the potential effect of radiation treatment on the LINE1 methylation level. Standard deviation between technical triplicates is indicated in the chart. Difference in the LINE1 methylation between untreated and irradiated sample was analyzed, as well as potential further effect of radiation in combination-treated organoids compared to DAC-treated organoids.*

To investigate potential locus specific changes in DNA methylation following radiation, we performed a pilot experiment to assess genome-wide DNA methylation using Illumina Infinium® Methylation EPIC arrays.

Differential methylation analysis between untreated (TP17) and irradiated samples

Although no apparent effects on DNA methylation were observed after analyzing LINE1 methylation levels by performing MethyLight experiments, results obtained after the Illumina Infinium® Methylation EPIC array indicated specific changes. Samples were kindly analyzed by Raheleh Sheibani, PhD. Firstly, irradiated (TP17 + 1Gy radiation) and the untreated sample (TP17) were compared.

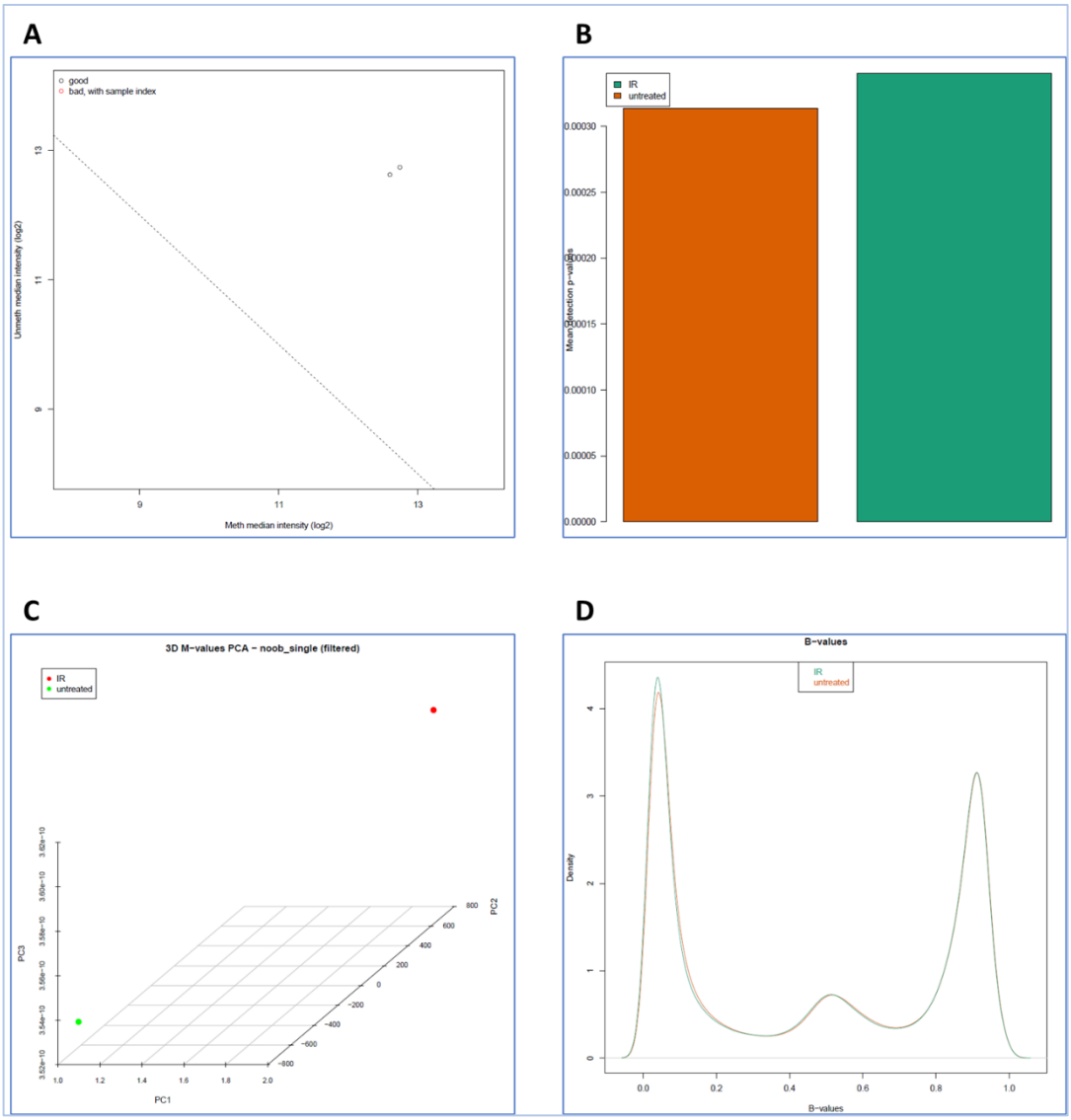

Figure 22. Assessment of DNA methylation changes upon radiation between irradiated and untreated samples. ***A*** *– Quality control plot indicating that both of samples are above the threshold, showing the good quality of both samples.* ***B –*** *The bar plot shows small mean-detection p-values, suggesting the high probability of significance of the results.* ***C -*** *The PCA plot shows no clustering of analyzed samples.* ***D –*** *Density plot with the depicted distribution of beta values after normalization.*

The quality control plots shown in *Figures 22A* and *22B* indicate the satisfactory quality of both samples used in this analysis. *Figure 22A* represents the median intensity plot where log values of median intensity of methylated and unmethylated channels are along the x- and y-axis, respectively. None of our samples fall under the threshold line, indicating their good quality. *Figure 22B* represents average detection p-values, summarizing the signal quality across all the probes in each sample. A small detection p-value of our samples indicates that measured intensity is very likely to be significant and not the background noise. In *Figure 22C,* the PCA (principal component analysis) plot is represented, showing that irradiated and untreated samples do not cluster together, suggesting a difference in their CpG methylation patterns. Finally, *Figure 22D* depicts a distribution of beta values after the normalization. The heatmap below (*see Figure 23*) depicts the top 1% of most variable probes (β-values). Distinct hypomethylated and hypermethylated clusters in the irradiated sample compared to the untreated sample can be seen in the supervised clustering. A clear indication of the radiation effect on the CpG methylation pattern suggested that radiation affects DNA methylation to a certain point.

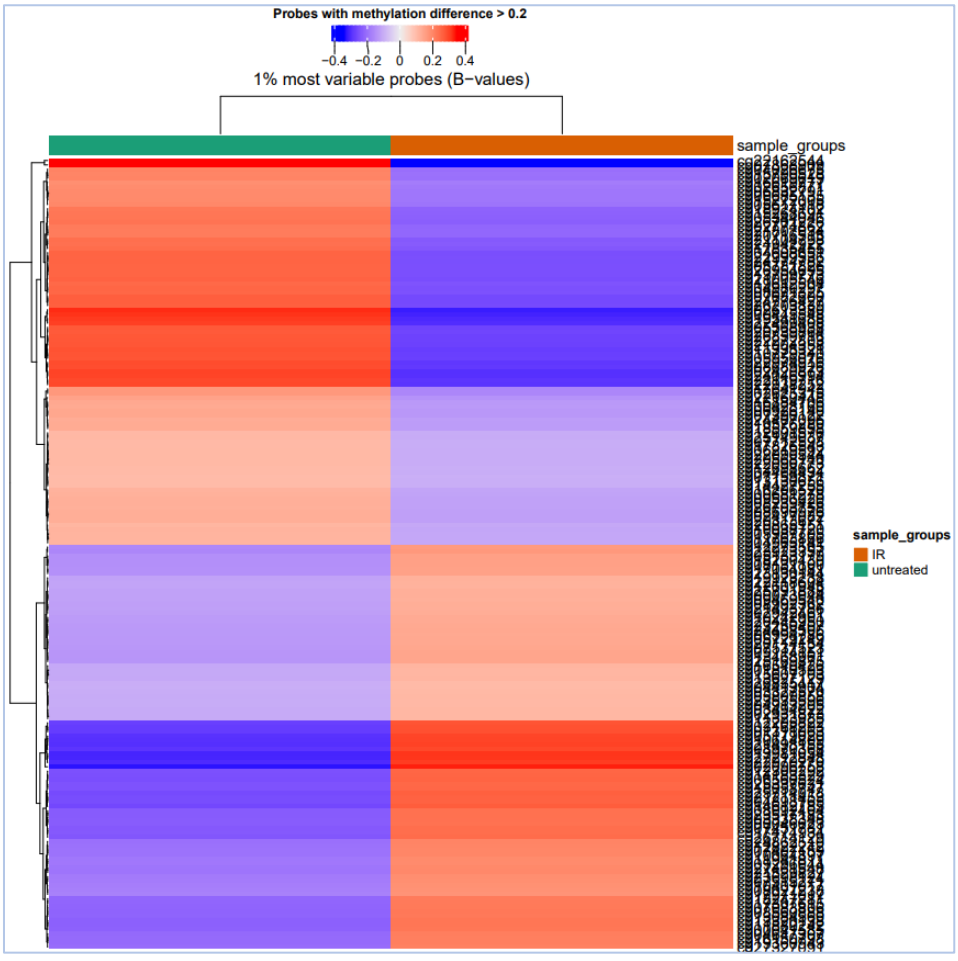

Figure 23. Supervised hierarchical clustering of top 1000 significant differentially methylated probes. *Comparison between untreated and radiation-treated samples. Hypermethylated probes are depicted in red, hypomethylated probes in blue (Illumina Infinium MethylationEPIC Bead Chip array, mean β-value differences > 0.2). Radiation seems to affect DNA methylation to a certain point. There is a clear indication of the radiation effect on the CpG DNA methylation pattern.*

Differential methylation analysis between DAC- and combination-treated samples

Similarly, we performed a comparison between DAC- and combination-treated samples. The data obtained after analysis indicated a further effect of radiation on DNA methylation, despite the apparent impact of the demethylating agent Decitabine. Charts shown in *Figures 24A, 24B,* and *24C* indicate the satisfactory quality of samples, low detection p-value indicating high likelihood of significance and a clear separation of sample groups in the PCA plot. Since β-value density did not change upon radiation treatment in neither 22D nor 24D figure, under these conditions, we did not observe any global effect despite some impact on DNA methylation.

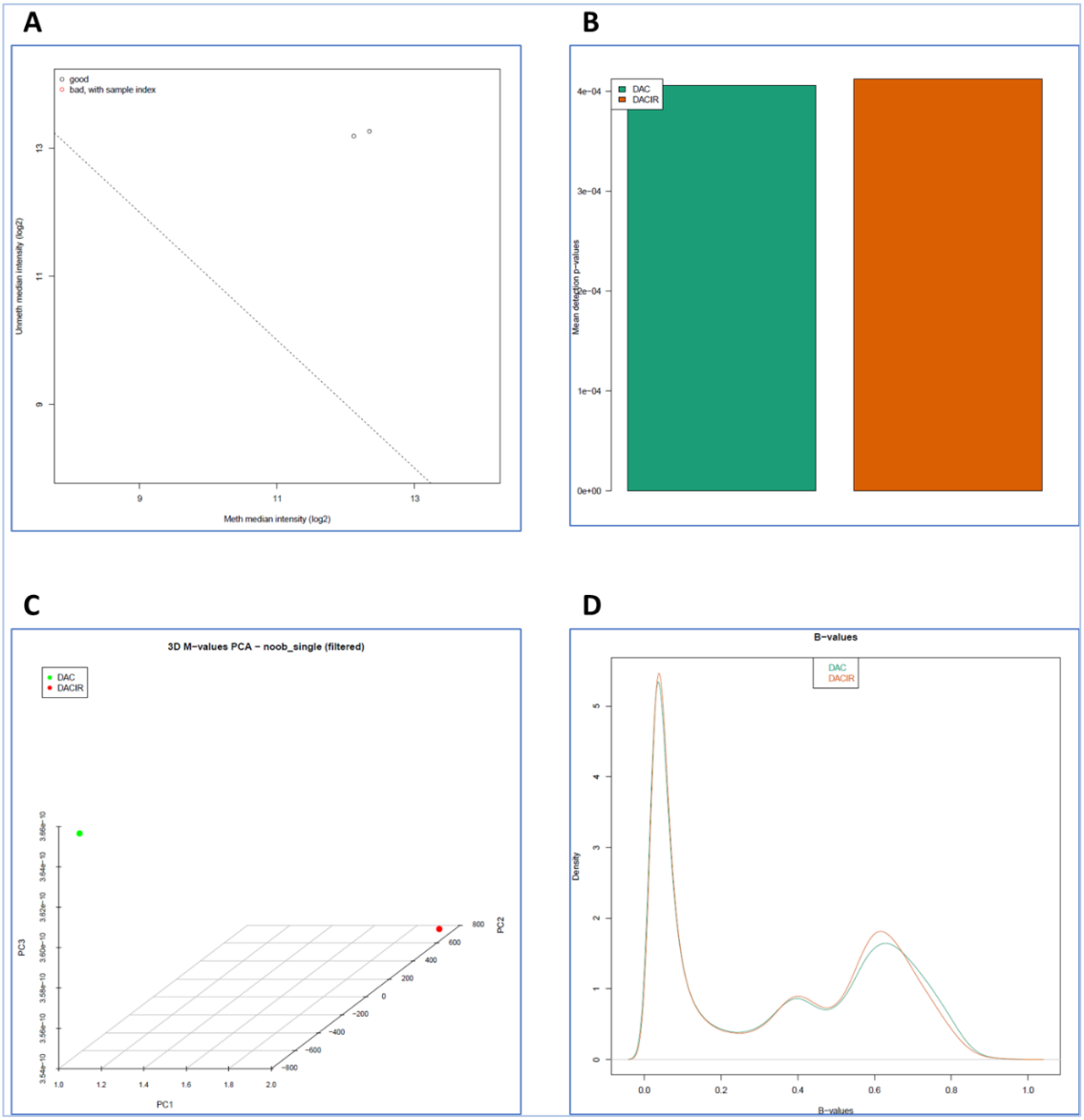

Figure 24. Assessment of DNA methylation changes upon radiation between DAC- and combination-treated samples. ***A*** *– Quality control plot indicating the good quality of both samples.* ***B*** *– The bar plot shows mean-detection p-values being < 0.05.* ***C*** *- The PCA plot shows the distant clustering of analyzed samples.* ***D*** *– Density plot with the depicted distribution of beta values density after normalization indicates an important shift upon DAC treatment.*

Figure 24D is showing a clear shift in the bimodal distribution of DNA methylation from fully methylated CpG sites to lower methylation, observed upon DAC treatment. If compared to untreated samples depicted in *Figure 22D*, a clear shift of highly methylated CpG sites towards lower methylation from around 1.0 to values around 0.6 after DAC treatment can be noted. However, this was to be expected considering the known effects of DAC on DNA methylation. Nevertheless, the heatmap (*see Figure 25*) again referred to distinct hypomethylated and hypermethylated clusters in the combination-treated sample compared to the DAC-treated sample, indicating certain changes that we plan to investigate further. Finally, since only one replicate per group was included, the possibility of the presence of false-positive/negative differences cannot be excluded. Therefore, future studies will analyze more replicates per group.

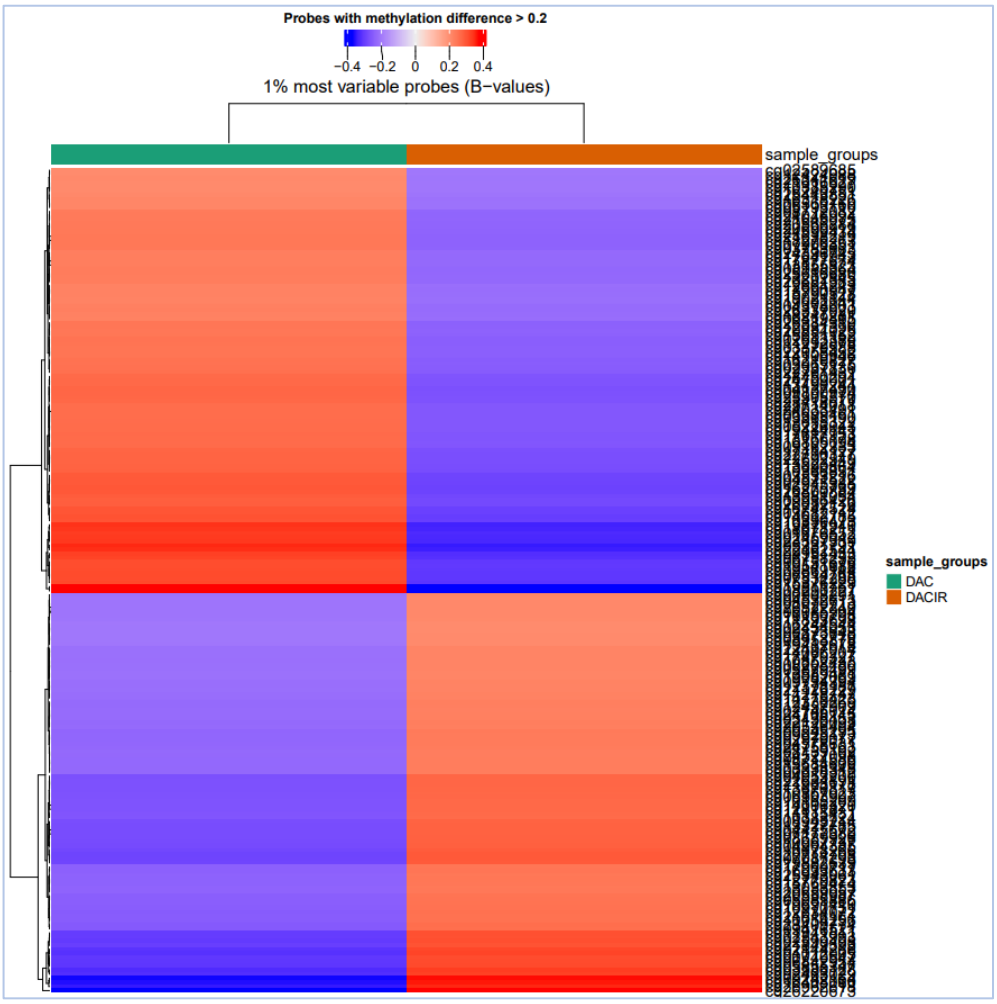

Figure 25. Supervised hierarchical clustering of top 1000 significant differentially methylated probes. *Comparison between DAC- and combination-treated samples. Hypermethylated probes are depicted in red, hypomethylated probes in blue (Illumina Infinium MethylationEPIC Bead Chip array, mean β-value differences > 0.2). Combinational treatment seems to have the effect on DNA methylation.*

Timepoint experiments – LINE1 methylation

Next, we aimed to analyze potential long-term effects of radiation on global DNA methylation. *Figure 26* tracks the morphological changes of organoids and shows the brightfield images taken on days 0, 5, 10, and 20. These were the crucial time points set for this experiment, briefly depicted in *Figure 8*, in *Material and Methods*. Importantly, day 0 is the day when radiation treatment was performed. We observed an apparent effect of both doses of radiotherapy on the density and size of RC1 organoids, which is also shown in *Figure 27*, representing cells/µL counted on day 5 for all three different conditions.

Both figures clearly show how the number of organoids decreased upon radiation and was much lower than untreated control on day 5. However, due to the clear and extreme effect of the 12 Gy radiation on the organoids, at the time point 20 days, almost no viable cells were spotted, and consequently, harvesting was not possible.

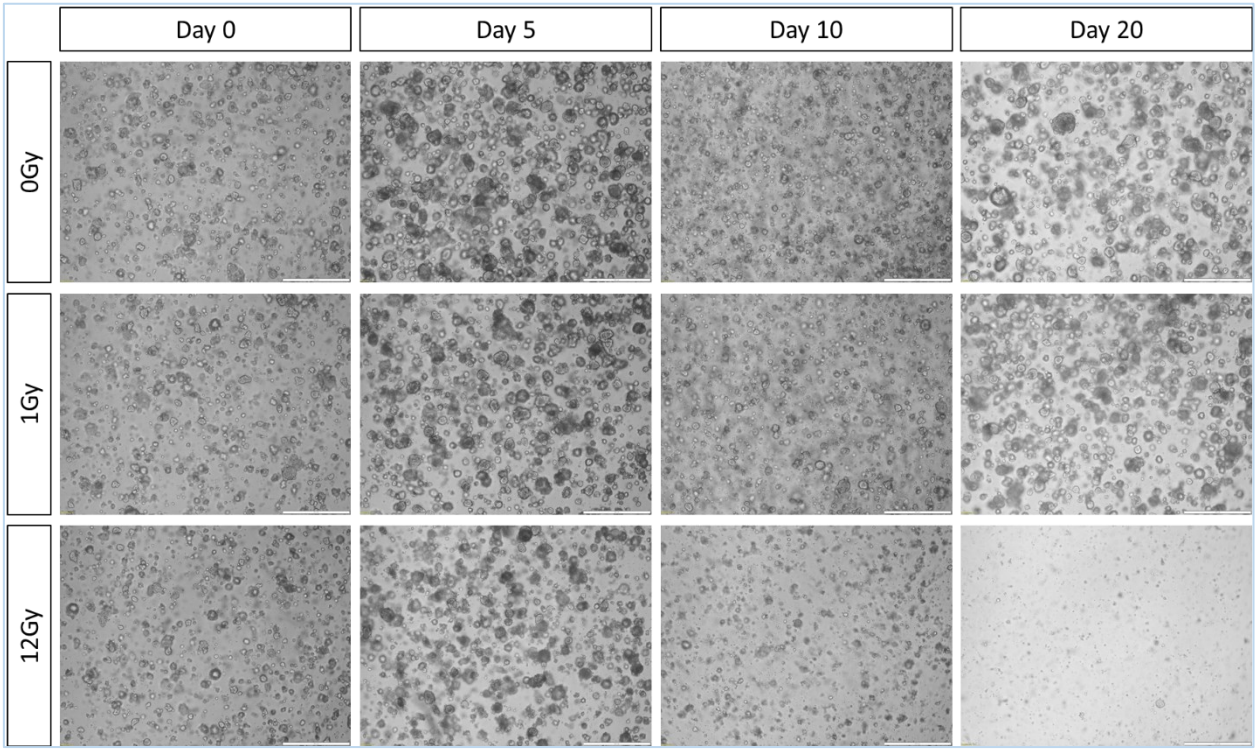

Figure 26. Brightfield images (scale bar: 500 µM) showing the effect of low- and high-dose radiotherapy on RC1 organoids*. Images taken on day 0 indicate the same organoid density in all three conditions before the treatment. These brightfield images of RC1 organoid line treated with different doses of radiation were taken on several time points, in order to track their density and morphological changes.*

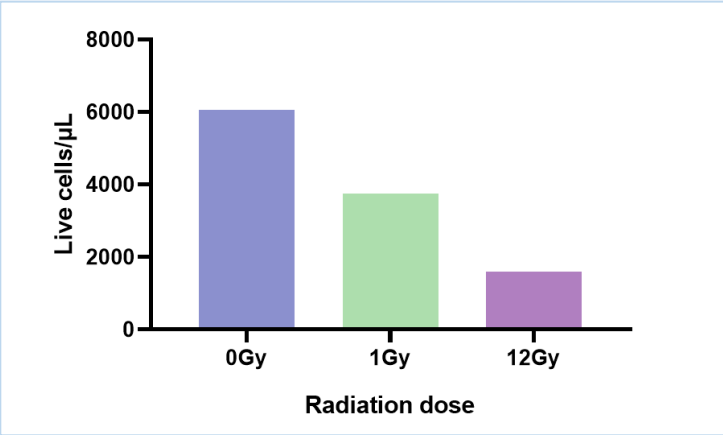

Figure 27. Counted live cells/µL at day 5 after the treatment. *Number of live cells/µL measured on day 5 after the radiation treatment was plotted in the chart in order to observe the effect of radiation on cell viability of RC1.*

No significant changes in LINE1 DNA methylation were observed upon radiation on time points 5, 10, and 20, as shown in *Figure 28*. As stated before, 12-Gy-treated organoids were not harvested at day 20 due to the low numbers of live cells. Therefore, we could not include this condition in the analysis.

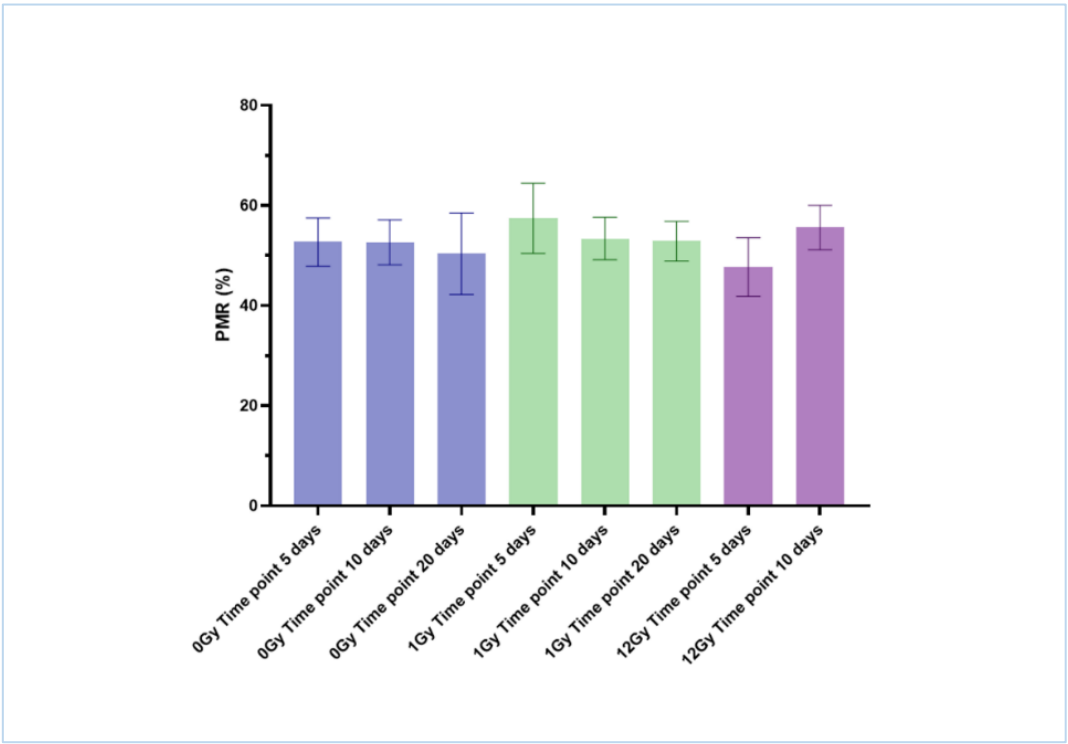

Figure 28. No significant change in level of LINE1 DNA methylation at different time points after the radiation treatment was observed. *Statistical significance was determined by Ordinary one-way ANOVA and Turkey's Multiple Comparisons Analysis of raw data. However, no significant changes were observed. Standard deviation between technical triplicates is included in the chart.*

In the case of CRC2, 12Gy-treated organoids on days 10 and 20 could not be harvested due to the low cell number. *Figure 29* represents brightfield images taken on the defined time points. Importantly, it was concluded that the CRC2 organoid line has a significantly lower level of LINE1 methylation compared to the RC1, which can be seen in *Figure 30.*

However, in line with the previous organoid line, we did not observe any changes in LINE1 methylation levels at different time points after low- and high-dose treatment, compared to the untreated control (*see Figure 31*), despite the apparent effect of radiation on their density and morphology (*see Figure 29)*.

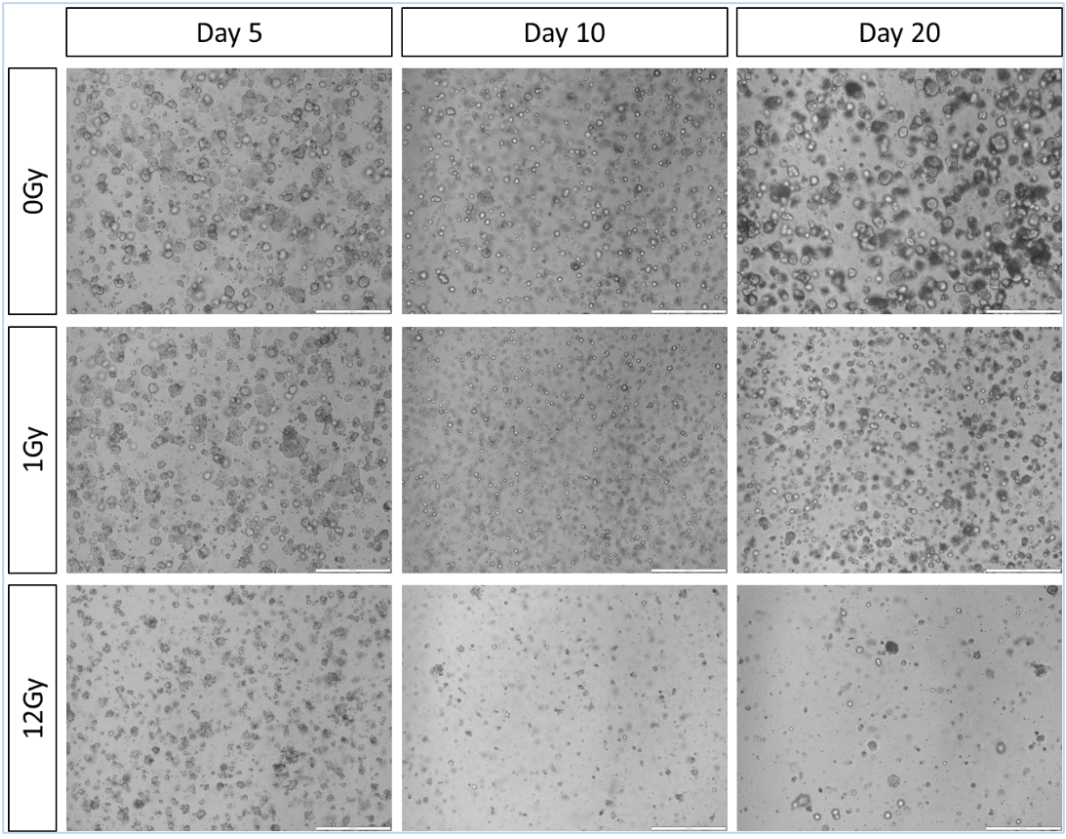

Figure 29. Brightfield images (scale bar: 500 µM) showing the effect of low- and high-dose radiotherapy on CRC2 organoids*. These brightfield images of CRC2 organoid line treated with different doses of radiation were taken on several time points, in order to track their density and morphological changes.*

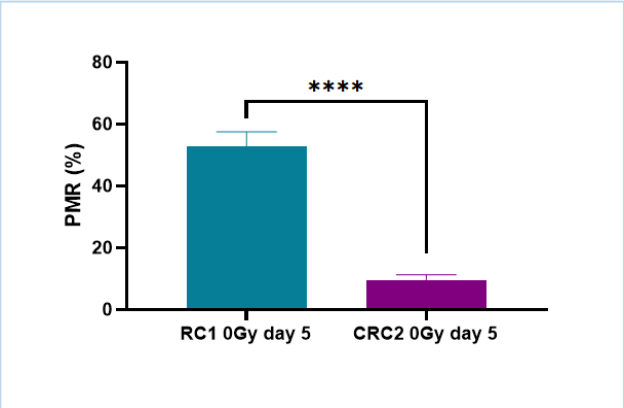

Figure 30. Chart showing a significant (****) difference in LINE1 methylation level between RC1 and CRC2 organoid lines*. *PMR (%) of untreated RC1 organoid line at day 5 after the radiation was compared to the value of PMR (%) of CRC2 organoid line at the same time point, in order to compare the level of LINE1 methylation between these two organoid lines. Raw data was analyzed. Statistical analysis done by t-test, ****P <0.0001.*

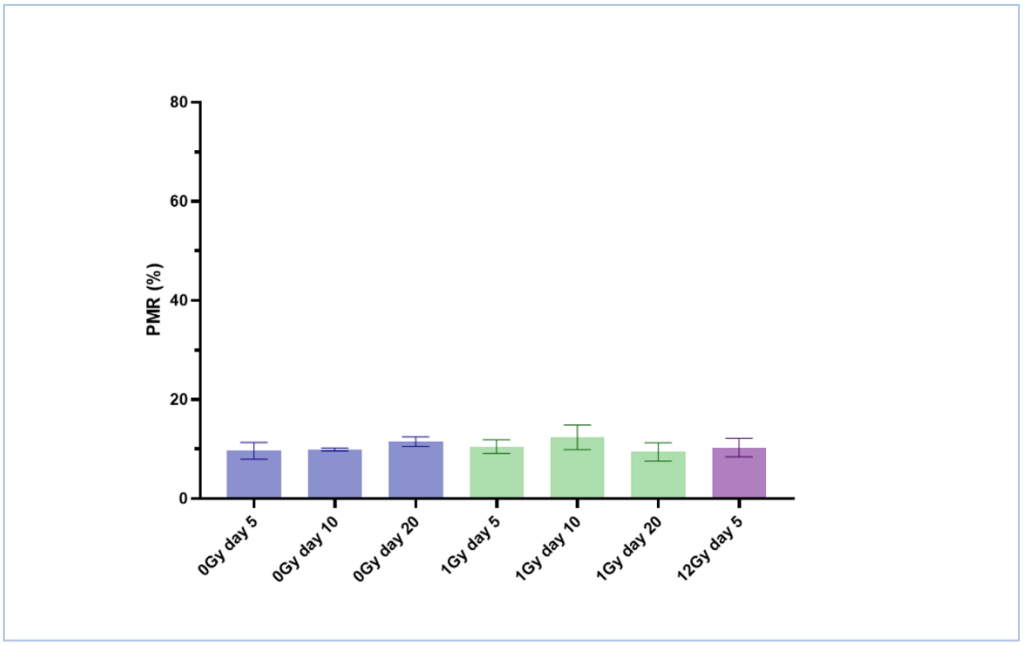

Figure 31. Level of LINE1 DNA methylation at different time points after the radiation treatment of CRC2 (shown as PMR %) does not indicate any significant effect of radiotherapy. *Statistical significance was determined by Ordinary one-way ANOVA and Turkey's Multiple Comparisons Analysis of raw data. However, no significant changes were observed. Standard deviation between technical triplicates is indicated in the chart.*

.

Persistent organoids

Further cultivation and expansion of the almost eradicated 12Gy-treated RC1 organoid line led to the establishment of a potentially persistent organoid line.

As shown in *Figure 32*, two weeks after the time point when almost no cells were observed, organoids were already formed. After two splitting steps and approximately one month later (day 64), it was concluded that this line was successfully established. This line will be further expanded and characterized.

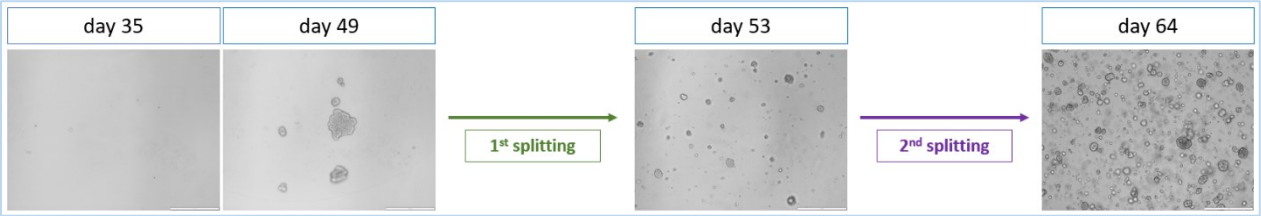

Figure 32. Cultivation of 'persistent RC1 organoid line' over time until the time point when we concluded that we successfully established this line. *These images were taken in order to track the growth and the progress of the establishment of potentially persistent RC1 organoid line (scale bar: 500 µM).*

Similarly, a 12Gy-pretreated CRC2 organoid line was cultivated until fully recovered (after ~ 2 weeks). However, since we showed that this organoid line is more resistant to radiation therapy, we assume that this radiation dose is not a high-dose treatment for this organoid line. Therefore, this pretreated CRC2 organoid line is not hypothesized to be persistent.

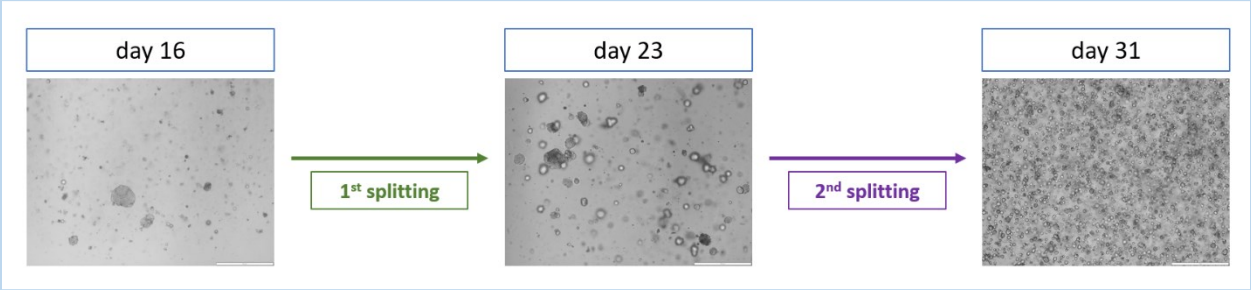

Figure 33. Cultivation of 'pretreated CRC2 organoid line' until the conclusion that this line was successfully recovered*. These images were taken in order to track the growth and the progress of the recovery of 12Gy-pretreated CRC2 organoid line (scale bar: 500 µM).*

Comparing the radiation response of pretreated organoid lines compared to untreated control

This experiment was performed to compare the sensitivity towards radiation after the lines were already pre-irradiated. To do so, we included untreated and 1Gy-/12Gy-pretreated CRC2 organoids and treated them with the same doses as in regular radiation response experiments. Importantly, the pretreatment was performed only once, and organoids were left for the two-week-long recovery before the following treatment. Our results (*see Figure 34*) did not indicate any difference in the radiation response.

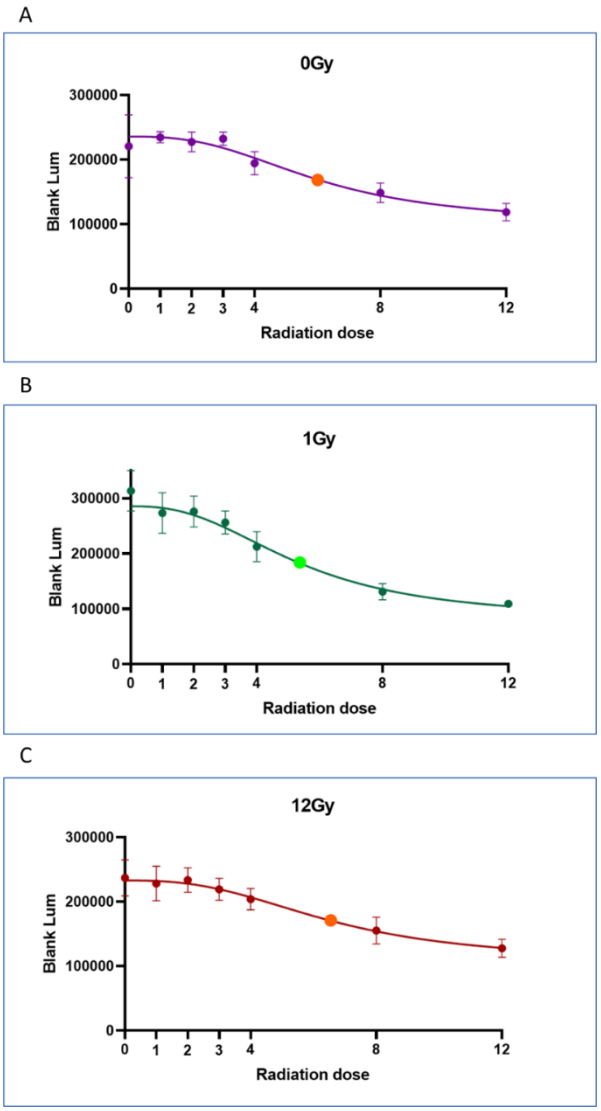

Figure 34. Comparing radiation response curves of pretreated CRC2 organoids to untreated control. *We could not observe any major difference between response of untreated* ***(A)****, 1Gy-* ***(B)*** *and 12Gy-* ***(C)*** *pretreated organoids. The Curve Fittings with Nonlinear Regression were generated using GraphPad Prism (the used equation: "[Inhibitor] vs. response -- Variable slope – four parameters"). Standard deviations between technical triplicates are also indicated in the chart.*

Discussion

The literature already suggested the mutual correlation between epigenetics and radiotherapy response in various cancer types, including colorectal carcinoma [38,39]. Furthermore, recent studies have emphasized the potential effect of radiotherapy on epigenetic alterations that could lead to the acquirement of radioresistant phenotypes. However, introduced alterations could potentially be reversed by pretreatment with epigenetic drugs. Therefore, this therapeutic approach could help in the resensitization of the patients [40]. Already in 2002, Kim et al. reported a correlation between hypermethylation of the *ATM* (Ataxia Telangiectasia Mutated) promoter and radioresistance. Strikingly, treatment with 5-azacytidine reversed hypermethylation, induced the expression of ATM to normal levels, and restored sensitivity to radiation [41].

Furthermore, *MGMT* promoter hypermethylation was reported to be a predictive biomarker for radiotherapy response in some tumor entities. Nevertheless, in some other cancers, its hypermethylation was correlated with poor prognosis after the treatment. *MGMT* encodes for a crucial DNA repair protein. In addition to *ATM* and *MGMT*, several other methylation markers were suggested to be associated with response to radiotherapy [40,42–44]. However, despite growing evidence about the link between epigenetic alterations and sensitivity to radiation, there are still many remaining questions to be answered. Nevertheless, due to its high importance for cancer research and clinics, this topic has to be further explored.

This project aims to investigate the reciprocal connection between radiotherapy and DNA methylation. Since it is still highly understudied, we seek to examine the effect of radiation on DNA methylation itself. On the other hand, we aim to explore the potential benefit of Decitabine pretreatment before irradiation. Epigenetic drugs have already been reported as possible resensitizers. For instance, 5-azacytidine was reported to lead to increased radiosensitivity in several tumor cell lines, including colorectal cancer. Similar association was already reported for DAC pretreatment [40,45,46].

The project was newly established with my Master's Thesis Project as a starting point. Since it was impossible to cover all previously explained aims within my thesis, we have defined three work packages (see Work Packages of the Master Thesis Project) that were important to set a stage for the rest of the project.

Corning® Matrigel® was identified as the most effective growth-supporting BME matrix

Based on our results, we could conclude that Corning® Matrigel® is the most favorable BME matrix for CRC1 and CRC2 lines. Importantly, brightfield images shown in the *Results* were not quantified. For the more precise estimation, quantification of the pictures would be necessary.

We have performed the same analysis for healthy and metastatic organoid lines. We did not include these lines in this project, so the data is not enclosed. Nevertheless, the results show that Corning® Matrigel® is the most efficient in growth support among all tested lines. Hence, we were using it throughout our experiments whenever this was possible. Due to the issues with production and delivery, in some experiments, we used Gibco™ Geltrex™. However, we defined Corning® Matrigel® as a desirable BME matrix to use.

CRC PDOs have been used successfully for sensitivity estimation towards different anticancer therapies

The first two work packages defined for my Master's Thesis Project were to determine sensitivity curves of PDO lines towards Decitabine and radiation treatment. These sensitivity curves were necessary as a start point for any other performed experiment. Firstly, we wanted to investigate whether we could identify different response rates among our organoid lines. Loan Tran, MSc, already established decitabine drug screening. Together we performed several experiments to determine the sensitivity of our organoid lines towards this DNMTi. As a result of the entire screening, we could distinguish between sensitive (IC50 < 1 μM), median-sensitive (1 μM < IC50 < 2 μM), and resistant organoids (IC50 > 2 μM). Based on this grouping, we found the lines included in my Master's Thesis project to be resistant. IC50 values were important to determine the desired concentrations for low-dose treatments used in further experiments for all lines included.

Similarly, I have established a protocol for radiation response curve determination. Again, we could see a difference in response among different PDOs, and we identified radio-resistant and radio-sensitive lines. Another critical purpose of sensitivity estimation in our project was to define low- and high-dose treatments for these therapies among our organoid lines. This was important because all further experiments required either high- or low-dose treatment to evaluate their effect on our organoids.

While Decitabine treatments were successfully finalized for all three organoid lines, the radiation response curve is still to be repeated due to the technical issues we faced while performing the experiment. In case of CRC1 organoid line, high standard deviations indicate that the replicates were not as consistent as in previous experiments. Additionally, the level of luminescence was much lower than the level measured for the other two organoid lines. Therefore, we could conclude that for CRC1, optimization is required since its growth rate differs from other lines. As already described in Material and Methods, the same starting number of cells/well is used for every experiment to ensure that experiments are comparable. Ultimately, the observed difference in density and morphology shows that organoids derived from different patients behave and grow distinctly. However, based on this experiment and the preliminary chart, we could assume that this line is highly resistant to radiotherapy. This would be expected since this line was derived from

the biopsy of the patient pretreated with radiotherapy. Additionally, this line carries a *TP53* mutation, which is an indicator of radioresistance. However, due to technical issues and not conclusive data, this experiment will be repeated in the future.

Nevertheless, our results align with other literature that indicates that PDOs can be used successfully to estimate sensitivity towards various cancer therapies and predict patients' responses, which is why this technology is an eminent promise for personalized medicine. The literature already reported valuable advantages of using PDOs for drug screening assays compared to previously used approaches [47–49]. Pasch et al. demonstrated the ability of PDOs to maintain the features of the tissue of origin and to predict the sensitivity towards chemo- and radiotherapy. The study included PDOs derived from various cancer tissue types and patients with diverse molecular and phenotypic characteristics. They have shown that PDOs can maintain these critical features through passages and reflect the patient's profile. Furthermore, the ability to predict a therapeutic response again suggested their great promise [32].

Patient-derived rectal cancer organoids were already suggested to be a suitable and promising tool in the determination of sensitivity towards chemotherapy, but also irradiation. In this study, Yao et al. also estimated the response curves based on the morphology of organoids and viability measured with the CellTiter-Glo 3D cell viability assay. These methods were used to group the lines into radio-resistant and -sensitive. The authors compared obtained data to clinical outcomes of the patients and proved high reliability of their results and a great promise of organoid technology in estimating radiation responses [36]. In order to investigate whether the estimated sensitivity of our organoid lines represents the patients, this study would have to be expanded and compared to the clinical data. Nevertheless, the results gained so far showed that we can identify different response rates for both Decitabine and radiation therapy.

Decitabine pretreatment might increase the rate of apoptosis upon radiotherapy

Our experiments aimed to tackle the potential benefit of DAC pretreatment on the sensitivity towards radiation. We treated the RC1 PDO line with either Decitabine/radiation alone or combined in the first experiment. In the case of combinational treatment, organoids were treated with DAC prior to the radiation exposure to explore the potential effect of DAC as a radiosensitizer.

Jiang et al. have already reported that the DNMT inhibitor, 5-azacytidine (5-azaC), induces the increased level of radiation-induced apoptosis and therefore mediates radiosensitizing effects in nasopharyngeal carcinoma cell lines CNE2 and SUNE1. At the same time, no significant difference in the level of apoptosis of 5-azaC treated cells compared to untreated control was observed. Strikingly, they showed that the reduction in methylation levels has led to increased mRNA expression of crucial apoptosis-associated tumor suppressors that can lead to the induction of apoptotic cell death. At the same time, the authors did not report any changes in the number of

γ.H2A.X foci. Therefore, DNMT inhibitors were suggested to resensitize NPC cancer cells by changing the DNA methylation status and reactivating tumor suppressor genes that play a pivotal role in apoptosis pathways [27].

Even though our immunofluorescence figures were not quantified, and this aspect was not further analyzed, our results also indicated no change in the level of γ.H2A.X foci among DAC pretreated organoids. Still, the results suggested that there might be an effect on the apoptosis levels. In order to explore this further, we plan to perform apoptosis assays that would allow us a more straightforward quantification of its level. This would help us conclude whether pretreatment leads to an increased apoptosis rate indeed and would help us set a stage for further analysis.

Radiation treatment induced the changes in DNA methylation pattern

We aimed to investigate the impact of radiotherapy on the epigenome. Studies have already reported the changes in global DNA methylation after the radiation. Still, they suggest that this effect is dependent on several things, including period and dose of the radiation, cell/tissue type, and postirradiation time. Therefore, we had to define low- and high-dose doses among our organoid lines. For example, Goetz et al. have previously shown that 1 Gy radiation dose leads to a different effect in RKO human CRC cells (DNA hypomethylation) compared to LINE1 hypermethylation reported in AG01522 primary human diploid skin fibroblasts [28,29].

Literature also reports diverse consequences of radiation on DNA methylation levels. While some reported decreases in DNA methylation, other groups have found DNA hypermethylation happening after various radiation doses, ranging up to 10 Gy. Consequently, all these diverse approaches in an experimental set-up, including different postirradiation time points, make it difficult to compare the results [50].

In order to tackle this question, we did several experiments. In our first experiment, we analyzed the methylation status of LINE1 elements. Since they comprise a significantly large part of our genome, analysis of the methylation status of LINE1 elements can be used as a marker in the estimation of global DNA methylation levels [17,25,28,29,51]. The results did not show any effect of the radiation on the LINE1 DNA methylation, suggesting no change on the global level as well. However, we sent these samples for Illumina Infinium® Methylation EPIC array.

Based on the results, we could see an apparent effect of radiotherapy on DNA methylation when comparing non-irradiated and irradiated samples. This was also reported for DAC-pretreated organoids, where global demethylation already occurred due to the effect of this DNMTi. However, as explained in the Material and Methods, DAC-only treated organoids were harvested four days before irradiated organoids afterward. Therefore, we cannot claim that this difference is only due to radiation treatment because an extended period after treatment with DNMTi could

have influenced the methylation level. Further analysis will also include another control that would be treated with DAC but harvested simultaneously as the sample treated with both therapies.

As a shortcoming for this analysis, I should point out that we included only one sample per condition. However, this experiment aimed to tackle this question and give us a lead about the possible effect of radiotherapy on DNA methylation. Despite not being conclusive, these results indicated a possible effect of radiation. However, β-values density did not change upon radiation treatment, suggesting no global impact on DNA methylation. Therefore, our data do not imply a global, but rather a local change.

Furthermore, we performed Timepoint Determination experiments to ensure that the timepoint when low-/high-dose radiation induces changes in methylation level was not missed. However, the results obtained did not reveal any effect on the LINE1 methylation level, suggesting no global impact. One should consider that estimation of LINE1 methylation level is not the most sensitive nor accurate method available.

Potentially persistent organoid line was successfully established

High-dose treatment (12 Gy) of the RC1 organoids, which we found to be sensitive compared to others, affected their growth and viability, leading almost to their eradication. Nevertheless, few viable cells that survived this treatment were cultivated and expanded only. A potentially persistent organoid line was successfully established after two weeks of cultivation and two passaging steps. In addition to the number of successfully grown organoids, at this time point, we observed that this line started recovering from the treatment. Splitting was immensely challenging the first two times since the organoids were digested extremely fast and were very sensitive to the TrypLE digestion. However, during the third splitting, we concluded that they seem much more robust and can be further used for experimental setups and all the necessary cultivation steps, including freezing and thawing.

Even though persistence is yet to be explored, and this line is still to be characterized, it was derived from only a few cells that managed to survive the high-dose treatment. This was the crucial milestone of the entire project that added a new aspect to the whole story.

Persistent cancer cells are critical in cancer research since they cause unexpected tumor relapses. These cells might exist even prior to the therapy but may also be induced upon exposure to the treatment. Nevertheless, persistence allows them to survive the pressure of the treatment and give rise to new relapse of the tumor, and most likely, metastasis. Therefore, it is crucial to investigate their survival mechanisms further and find a way to detect and target these cells [52].

Similarly, the 12-Gy-treated CRC2 organoids were kept in culture and further expanded. However, since we showed that this organoid line is more resistant to radiation therapy, we assume that this

radiation dose is not a high-dose treatment for this organoid line. Nevertheless, it was decided to expand them further and include the CRC2 pretreated organoid line in the further analysis with the potentially persistent RC1 organoid line mentioned before.

Finally, the last experiment aimed to investigate whether the pretreatment led to increased radiation therapy resistance. The results obtained did not suggest any change in the treatment response. Nevertheless, this was just the pilot experiment, and this aspect will be further explained.

Conclusion and future prospective

This project aims to shed light on the correlation between radiotherapy and DNA methylation. Taken all together, our data so far confirm the potential of PDO technology and go in line with the reported advantages of this model in cancer research and drug screening. As previously stated, our organoid lines showed a diverse response towards both DAC and radiation treatment. Most importantly, technical replicates confirmed the reliability of our results. Therefore, we could have distinguished between more sensitive and resistant organoid lines for both treatments.

Despite its great potential, organoid technology has certain limitations. Therefore, our group is also focusing on expanding the capabilities of this model by establishing co-culture systems of tumor and healthy organoids with fibroblasts and immune cells. Considering the unquestioned importance of the microenvironment in all aspects of cancer biology and therapy, co-culture systems would be of great importance in exploring this project's research questions.

Furthermore, screened organoid lines showed diverse methylation patterns and levels of global DNA methylation between each other. Nevertheless, the methylation level of the same line remained the same after passaging steps, which confirms the great potential in using PDOs for DNA methylation analysis. Other epigenetic modifications also play a pivotal role in developing radioresistance. Therefore, despite focusing on DNA methylation, it is crucial to consider the crosstalk between different epigenetic mechanisms and their mutual role in cancer biology, including radiotherapy response. For instance, both microRNAs and histone modifications were suggested to be important in modulating radioresistance in different cancer types [53,54]. Therefore, one should keep in mind orchestrated manner of epigenetic mechanisms crosstalk in future studies.

Another important aspect for future studies is chemotherapy being essential for neoadjuvant chemoradiation. Neoadjuvant treatment can be given as either short-course radiotherapy or as chemoradiotherapy with 5-fluorouracil (5-FU) or capecitabine (an oral fluoro-pyrimidine) [3,55]. Hence, chemotherapy should not be excluded from such studies and is also planned to be incorporated in this project.

During my Master's Thesis Project, I performed several experiments to tackle the possible effect of irradiation on DNA methylation. Even though no global changes were reported, neither with low- nor high-dose treatments, results obtained after the Illumina Infinium® Methylation EPIC array indicated specific changes. However, since having only one sample per group is the drawback of this experiment, this is still to be further investigated.

Most importantly, I have cultivated and expanded only a few cells that have survived the high-dose radiation. We hypothesize that this established line might be persistent, and we aim to characterize it further. However, this added an entirely new aspect to the project that was not previously planned.

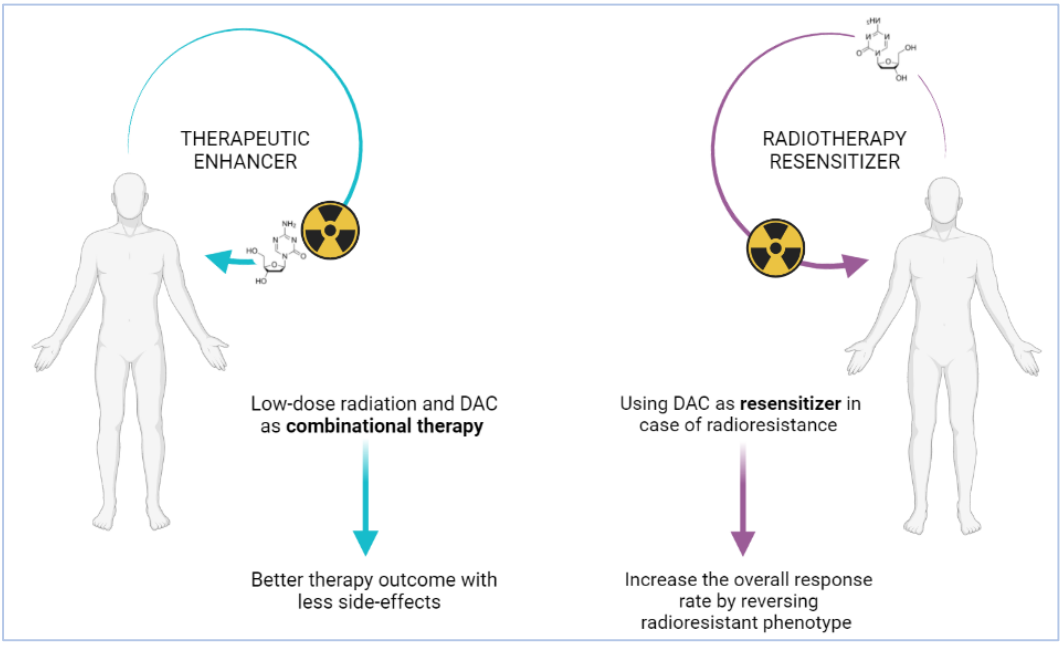

Figure 35. Expected outcomes of the project. *Decitabine might be beneficial in clinics as either a therapeutic enhancer (left) or radiotherapy resensitizer (right).*

As explained before, the project's biggest goal is to evaluate the potential beneficial role of Decitabine pretreatment on radiation response. The gained knowledge from this project will give insights into the potential role of Decitabine as a therapeutic enhancer or even as a resensitizer. In the first setting, clinicians might use low doses of both radiation and DAC to achieve a better response. As an enhancer, DAC might enable better therapeutical outcomes with fewer side effects to a patient. On the other hand, if the resensitizing ability is proven, DAC might reverse the resistant phenotype and increase the overall response rate. The project's expected outcomes can be found above, depicted in *Figure 35*.

Our results gained so far suggest that pretreatment with Decitabine induces apoptosis levels, which might lead to resensitization. However, we will evaluate this question further in the future.

In order to ensure financing for this newly established project, I gladly joined my supervisor, Loan Tran, MSc, in writing a grant proposal and submitting it for the Fund of the City of Vienna (StadtWien) for Innovative Interdisciplinary Cancer Research (Cancer Research Fund). Therefore, we secured financing for this project for the next two years. In this period, we will further examine all the above-mentioned research questions. As part of my work, I have managed to set a stage for further investigation and perform all the experiments that would lead this project further. We have shown a great potential of organoid technology in low-scale drug screens and in exploring DNA methylation. Finally, our data indicated the effect of radiotherapy on the epigenome and potential benefits of Decitabine pretreatment in the therapeutic setting. Most importantly, a new aspect of establishing persistent organoid lines might be of great importance for further investigation of tumor relapse and biomarker identification.

Literature

1. Statistik Austria. 31.05.2021. Available from: https://www.statistik.at/web_de/statistiken/menschen_und_gesellschaft/gesundheit/krebserkrankungen/dickdarm_enddarm/index.html.
2. Vuik, F. E. R. *et al.* Increasing incidence of colorectal cancer in young adults in Europe over the last 25 years. *Gut* 1820–1826 (2019) doi:10.1136/gutjnl-2018-317592.
3. Kuipers, E. J. *et al.* Colorectal cancer. *Nature Reviews Disease Primers* **1**, 1–25 (2015).
4. Rosato, V. *et al.* Risk factors for young-onset colorectal cancer. *Cancer Causes and Control* **24**, 335–341 (2013).
5. Guinney, J. *et al.* The consensus molecular subtypes of colorectal cancer. *Nature Medicine* **21**, 1350–1356 (2015).
6. Jung, G., Hernández-Illán, E., Moreira, L., Balaguer, F. & Goel, A. Epigenetics of colorectal cancer: biomarker and therapeutic potential. *Nature Reviews Gastroenterology and Hepatology* **17**, 111–130 (2020).
7. Dienstmann, R. *et al.* Consensus molecular subtypes and the evolution of precision medicine in colorectal cancer. *Nature Reviews Cancer* **17**, 79–92 (2017).
8. Glynne-Jones, R. *et al.* Rectal cancer: ESMO Clinical Practice Guidelines for diagnosis, treatment and follow-up. *Annals of Oncology* **28**, iv22–iv40 (2017).
9. Hardiman, K. M. *et al.* Intra-tumor genetic heterogeneity in rectal cancer. *Laboratory Investigation* **96**, 4–15 (2016).
10. Exner, R. *et al.* Potential of DNA methylation in rectal cancer as diagnostic and prognostic biomarkers. *BRITISH JOURNAL OF CANCER* 1035–1045 (2015) doi:10.1038/bjc.2015.303.
11. Frydrych, L. M. *et al.* Rectal cancer sub-clones respond differentially to neoadjuvant therapy. *Neoplasia (United States)* **21**, 1051–1062 (2019).
12. Keller, D. S., Berho, M., Perez, R. O., Wexner, S. D. & Chand, M. The multidisciplinary management of rectal cancer. *Nature Reviews Gastroenterology and Hepatology* **17**, 414–429 (2020).
13. Buckley, A. M., Lynam-Lennon, N., O'Neill, H. & O'Sullivan, J. Targeting hallmarks of cancer to enhance radiosensitivity in gastrointestinal cancers. *Nature Reviews Gastroenterology and Hepatology* **17**, 298–313 (2020).
14. Roeder, F., Meldolesi, E., Gerum, S., Valentini, V. & Rödel, C. Recent advances in (chemo-)radiation therapy for rectal cancer: a comprehensive review. *Radiation Oncology* **15**, 1–21 (2020).
15. Hanahan, D. & Weinberg, R. A. *The Hallmarks of Cancer*. *Cell* vol. 100 (2000).

16. Hanahan, D. & Weinberg, R. A. Hallmarks of cancer: The next generation. *Cell* vol. 144 646–674 (2011).

17. Egger, G., Liang, G., Aparicio, A. & Jones, P. A. Epigenetics in human disease and prospects for epigenetic therapy. *Nature* **429**, 457–463 (2004).

18. Hanahan, D. Hallmarks of Cancer: New Dimensions. *Cancer Discovery* vol. 12 31–46 (2022).

19. Dillinger, T. *et al.* Identification of tumor tissue-derived DNA methylation biomarkers for the detection and therapy response evaluation of metastatic castration resistant prostate cancer in liquid biopsies. *Molecular Cancer* vol. 21 (2022).

20. Mosashvilli, D. *et al.* Global histone acetylation levels: Prognostic relevance in patients with renal cell carcinoma. *Cancer Science* **101**, 2664–2669 (2010).

21. Costello, J. F. *et al.* Aberrant CpG-island methylation has non-random and tumour-type-specific patterns. *Nature Genetics* **24**, 132–138 (2000).

22. Raha, P. Outcome of Combining Epigenetic Drugs with Other Treatments in the Clinic. *Medical Epigenetics* 799–826 (2016) doi:10.1016/B978-0-12-803239-8.00040-5.

23. Yu, G. *et al.* Low-dose decitabine enhances the effect of PD-1 blockade in colorectal cancer with microsatellite stability by re-modulating the tumor microenvironment. *Cellular and Molecular Immunology* **16**, 401–409 (2019).

24. Morel, D., Jeffery, D., Aspeslagh, S., Almouzni, G. & Postel-Vinay, S. Combining epigenetic drugs with other therapies for solid tumours — past lessons and future promise. *Nature Reviews Clinical Oncology* **17**, 91–107 (2020).

25. Weisenberger, D. J. *et al.* Analysis of repetitive element DNA methylation by MethyLight. *Nucleic Acids Research* **33**, 6823–6836 (2005).

26. Stresemann, C. & Lyko, F. Modes of action of the DNA methyltransferase inhibitors azacytidine and decitabine. *International Journal of Cancer* **123**, 8–13 (2008).

27. Jiang, W. *et al.* 5-azacytidine enhances the radiosensitivity of CNE2 and SUNE1 cells in vitro and in vivo possibly by altering DNA methylation. *PLoS ONE* **9**, 1–10 (2014).

28. Miousse, I. R., Kutanzi, K. R. & Koturbash, I. Effects of Ionizing Radiation on DNA Methylation: From Experimental Biology to Clinical Applications. *Int J Radiat Biol* **93**, 457–469 (2018).

29. Wilfried Goetz, M. N. M. M. and J. E. B. The Effect of Radiation Quality on Genomic DNA Methylation Profiles in Irradiated Human Cell Lines. *Radiation Research* **175**, 575–587 (2011).

30. Kim, J., Koo, B. K. & Knoblich, J. A. Human organoids: model systems for human biology and medicine. *Nature Reviews Molecular Cell Biology* vol. 21 571–584 (2020).

31. Qu, J., Kalyani, F. S., Liu, L., Cheng, T. & Chen, L. Tumor organoids: synergistic applications, current challenges, and future prospects in cancer therapy. *Cancer Communications* 1–23 (2021) doi:10.1002/cac2.12224.

32. Cheri A. Pasch1, Peter F. Favreau2, Alexander E. Yueh3, Christopher P. Babiarz3, A. A. *et al.* Patient-derived cancer organoid cultures to predict sensitivity to chemotherapy and radiation. *Clin Cancer Res.* **176**, 100–106 (2019).

33. Joshi, R. *et al.* The DNA methylation landscape of human cancer organoids available at the American type culture collection. *Epigenetics* **15**, 1167–1177 (2020).

34. Roerink, S. F. *et al.* Intra-tumour diversification in colorectal cancer at the single-cell level. *Nature* **556**, 437–462 (2018).

35. Kraiczy, J. *et al.* DNA methylation defines regional identity of human intestinal epithelial organoids and undergoes dynamic changes during development. *Gut* **68**, 49–61 (2019).

36. Yao, Y. *et al.* Patient-Derived Organoids Predict Chemoradiation Responses of Locally Advanced Rectal Cancer. *Cell Stem Cell* **26**, 17-26.e6 (2020).

37. edited by Jörg Tost. *DNA Methylation Methods and Protocols*. *Springer Protocols - Methods in Molecular Biology* (2009). doi:10.1002/9780470959824.ch2.

38. Hofstetter, B. *et al.* Impact of Genomic Methylation on Radiation Sensitivity of Colorectal Carcinoma. *International Journal of Radiation Oncology Biology Physics* **76**, 1512–1519 (2010).

39. Peitzsch, C. *et al.* An epigenetic reprogramming strategy to resensitize radioresistant prostate cancer cells. *Cancer Research* **76**, 2637–2651 (2016).

40. Smits, K. M. *et al.* Epigenetics in radiotherapy: Where are we heading? *Radiotherapy and Oncology* **111**, 168–177 (2014).

41. Kim, W. J., Vo, Q. N., Shrivastav, M., Lataxes, T. A. & Brown, K. D. Aberrant methylation of the ATM promoter correlates with increased radiosensitivity in a human colorectal tumor cell line. *Oncogene* **21**, 3864–3871 (2002).

42. Rivera, A. L. *et al.* MGMT promoter methylation is predictive of response to radiotherapy and prognostic in the absence of adjuvant alkylating chemotherapy for glioblastoma. *Neuro-Oncology* **12**, 116–121 (2010).

43. Dillinger, T. *et al.* Identification of tumor tissue-derived DNA methylation biomarkers for the detection and therapy response evaluation of metastatic castration resistant prostate cancer in liquid biopsies. *Molecular Cancer* **21**, 1–8 (2022).

44. Costa-Pinheiro, P., Montezuma, D., Henrique, R. & Jerónimo, C. Diagnostic and prognostic epigenetic biomarkers in cancer. *Epigenomics* **7**, 1003–1015 (2015).

45. Hofstetter, B. *et al.* Impact of Genomic Methylation on Radiation Sensitivity of Colorectal Carcinoma. *International Journal of Radiation Oncology Biology Physics* **76**, 1512–1519 (2010).

46. Qiu, H., Yashiro, M., Shinto, O., Matsuzaki, T. & Hirakawa, K. DNA methyltransferase inhibitor 5-aza-CdR enhances the radiosensitivity of gastric cancer cells. *Cancer Science* **100**, 181–188 (2009).

47. Van De Wetering, M. *et al.* Prospective derivation of a living organoid biobank of colorectal cancer patients. *Cell* **161**, 933–945 (2015).

48. Ooft, S. N. *et al.* Patient-derived organoids can predict response to chemotherapy in metastatic colorectal cancer patients. *Science Translational Medicine* **11**, 1–10 (2019).

49. Scognamiglio, G. *et al.* Patient-derived organoids as a potential model to predict response to PD-1/PD-L1 checkpoint inhibitors. *British Journal of Cancer* **121**, 979–982 (2019).

50. Michelle R. Newman, Pamela J. Sykes, Benjamin J. Blyth, Eva Bezak, Mark D. Lawrence, K. L. M. and R. J. O. The Methylation of DNA Repeat Elements is Sex-Dependent and Temporally Different in Response to X Radiation in Radiosensitive and Radioresistant Mouse Strains. *Radiation Research* **181**, 65–75 (2014).

51. Jung, G., Hernández-Illán, E., Moreira, L., Balaguer, F. & Goel, A. Epigenetics of colorectal cancer: biomarker and therapeutic potential. *Nature Reviews Gastroenterology and Hepatology* **17**, 111–130 (2020).

52. Shen, S., Vagner, S. & Robert, C. Persistent Cancer Cells: The Deadly Survivors. *Cell* **183**, 860–874 (2020).

53. Wu, Y., Pu, N., Su, W., Yang, X. & Xing, C. Downregulation of miR-1 in colorectal cancer promotes radioresistance and aggressive phenotypes. *Journal of Cancer* **11**, 4832–4840 (2020).

54. Macedo-Silva, C. *et al.* JmjC-KDMs KDM3A and KDM6B modulate radioresistance under hypoxic conditions in esophageal squamous cell carcinoma. *Cell Death and Disease* **11**, (2020).

55. Li, Y. *et al.* A review of neoadjuvant chemoradiotherapy for locally advanced rectal cancer. *International Journal of Biological Sciences* **12**, 1022–1031 (2016).